2010-01-01

Mechanical Loading Affects the Energy Metabolism of Intervertebral Disc Cells

Hanan Nirosha Fernando
University of Miami, hanan.fernando@gmail.com

UNIVERSITY OF MIAMI

MECHANICAL LOADING AFFECTS THE ENERGY METABOLISM OF INTERVERTEBRAL DISC CELLS

By

Hanan Nirosha Fernando

A THESIS

Submitted to the Faculty
of the University of Miami
in partial fulfillment of the requirements for
the degree of Master of Science

Coral Gables, Florida

June 2010

UNIVERSITY OF MIAMI

A thesis submitted in partial fulfillment of
the requirements for the degree of
Master of Science

MECHANICAL LOADING AFFECTS THE ENERGY METABOLISM OF INTERVERTEBRAL DISC CELLS

Hanan Nirosha Fernando

Approved:

Chun-Yuh (Charles) Huang, Ph. D. Assistant Professor of Biomedical Engineering	Terri A. Scandura, Ph. D. Dean of the Graduate School
Salahadin Abdi, M.D., Ph. D. Professor and Chief University of Miami Pain Center Dept. of Anesthesiology, Perioperative Med and Pain Management Miller School of Medicine	Weiyong Gu, Ph. D. Associate Professor of Biomedical Engineering

FERNANDO, HANAN NIROSHA (M.S., Biomedical Engineering)
(June 2010)

Mechanical Loading Affects the Energy
Metabolism of Intervertebral Disc Cells.

Abstract of a thesis at the University of Miami.

Thesis supervised by Professor Chun-Yuh (Charles) Huang.

No. of pages in text. (90)

Back pain is the second most common neurological ailment in the United States and the leading cause of pain and disability. More than 80% of the total US population experiences back-pain during their life time and the annual back pain related healthcare costs exceed 100 billion dollars. While the exact cause of low back pain (LBP) is still unknown, degeneration of the intervertebral disc (IVD) has been suggested as a primary contributor. IVD is the largest avascular tissue in the human body and it is composed of three integrated tissues (annulus fibrosus - AF, nucleus pulposus - NP and cartilaginous end plate - CEP). IVD functions as a shock-absorber during motion and provides flexibility to motion of the spine. Maintaining IVD tissue integrity is an energy demanding process. Studies have shown that mechanical loading affects cellular biosynthesis of IVD tissue and may also promote IVD degeneration. However the path to this effect is still unknown. We propose a link between mechanical loading and cell energy production which contributes to altered cellular biosynthesis. Thus, we investigated the effects of mechanical loading on IVD cell energy metabolism under various mechanical loading regimes.

Porcine AF and NP cells were isolated and seeded in 2% agarose at a 5,000,000 cells/mL cell density. A custom made bioreactor was used to conduct compression experiments. The experiment groups were: 15% static compression; 30% static compression; 0.1, 1 and 2 Hz dynamic compression at 15% strain magnitude. Experiment duration was 4 hr. ATP concentration in cell-agarose construct and culture media were measured using Luciferin-luciferase method to evaluate ATP production and ATP release from cells respectively. Lactate concentration in media was measured using lactate dehydrogenase enzymatic assay. Nitrite (stable metabolite of nitric oxide - NO) concentration in media was measured by Greiss Assay. DNA content per sample was measured using fluorometric assay. DNA content per sample was used as an internal control; all compressed samples were then normalized to unstrained control group.

ATP production of AF cells was up regulated by static and dynamic mechanical loading. Data suggests that AF cell response to mechanical loading is primarily loading amplitude dependent. NP cells exhibited an increased ATP production at 1 Hz dynamic loading but remained comparable to control samples at other tested conditions. AF cells produced an increase in NO production at 1-, 2 Hz dynamic loading. NO production of NP cells was up regulated by mechanical loading at all tested conditions. ATP release was up regulated at higher frequencies in AF cells. In addition to higher frequencies (1 Hz and 2 Hz) NP cell ATP release was also up regulated by 30% static compression. Thus, this study clearly illustrates that mechanical loading affects IVD cell energy production.

Acknowledgements

I would like to thank Dr. Huang for his guidance and patience throughout my time in his lab and giving me the opportunity to work on multiple exciting projects. I am truly grateful and honored that you have taken the time to make me a better researcher. I am also thankful to Dr. Cheung for introducing me to Dr. Huang and believing in me. I would like to thank Dr. Gu for his support and feedback on this project. I would also like to thank Dr. Abdi for his support and insight to this project.

I wish to extend a special thank you to Tai-Yi who has guided me and always been there for me. I know you have gone beyond your responsibilities to help me achieve my goals and I shall always be grateful for your advice and your friendship. I wish to thank Selma for keeping me sane during stressful times and Jessica for always being there for me. I wish to thank Daniel, Alicia, Andre, Nestor, Peter, Daniela, Chong and everyone else who have helped me along the way. You have all helped me in more ways than you may know, and I thank you for your support and friendship.

Lastly and most importantly, I would like to express my gratitude to my parents and my family for I believe my achievements would not have been possible without their dedication and sacrifices. I would like to thank my husband, Praneeth for his understanding, patience and continued support. I know I would not have reached this far without your persistent backing.

Finally I would like to say that this has been a wonderful experience. I have met people from different cultures and perceptions and all of you have changed my life for the better. I am grateful to know everyone I have met here and I will miss working with all of you.

TABLE OF CONTENTS

LIST OF FIGURES AND TABLES

Chapter 1: INTRODUCTION

Back pain is the second most common neurological ailment in the United States and is the leading cause of pain and disability. More than 80% of the total US population experiences back-pain during their lifetime. Direct and indirect annual health care related costs due to back pain exceed 100 billion dollars making it a significant socio-economic burden [1]. Despite its prevalence, our understanding of the disease process is poor. Degeneration of the intervertebral disc (IVD) has been suggested as a significant contributor to low-back pain (LBP), stimulating a significant interest in identifying the causes of IVD degeneration. Current treatments for LBP is limited and is not always successful and may in fact cause further damage to the spine [40,48,73].

Extracellular matrix (ECM) synthesis, which is critical to retain IVD tissue integrity, is an energy demanding process. Inefficient maintenance of IVD tissue matrix has been implicated in promoting tissue degeneration. Additionally, the IVD is constantly subjected to various mechanical loads due to movement of the spine. Therefore understanding IVD tissue regulation and its mechanobiology will facilitate in finding optimum treatments and preventive methods for disc degeneration and LBP. The objective of this study was to investigate the effects of mechanical loading on the energy metabolism of isolated IVD cells.

1.1: Structure, function and composition of IVD

The primary functions of spine include movement, load support and protection to the spinal cord. The human spine is made of 33 vertebral bodies, 22 of which are separated by intervertebral discs (IVD) [Figure 1- 1].

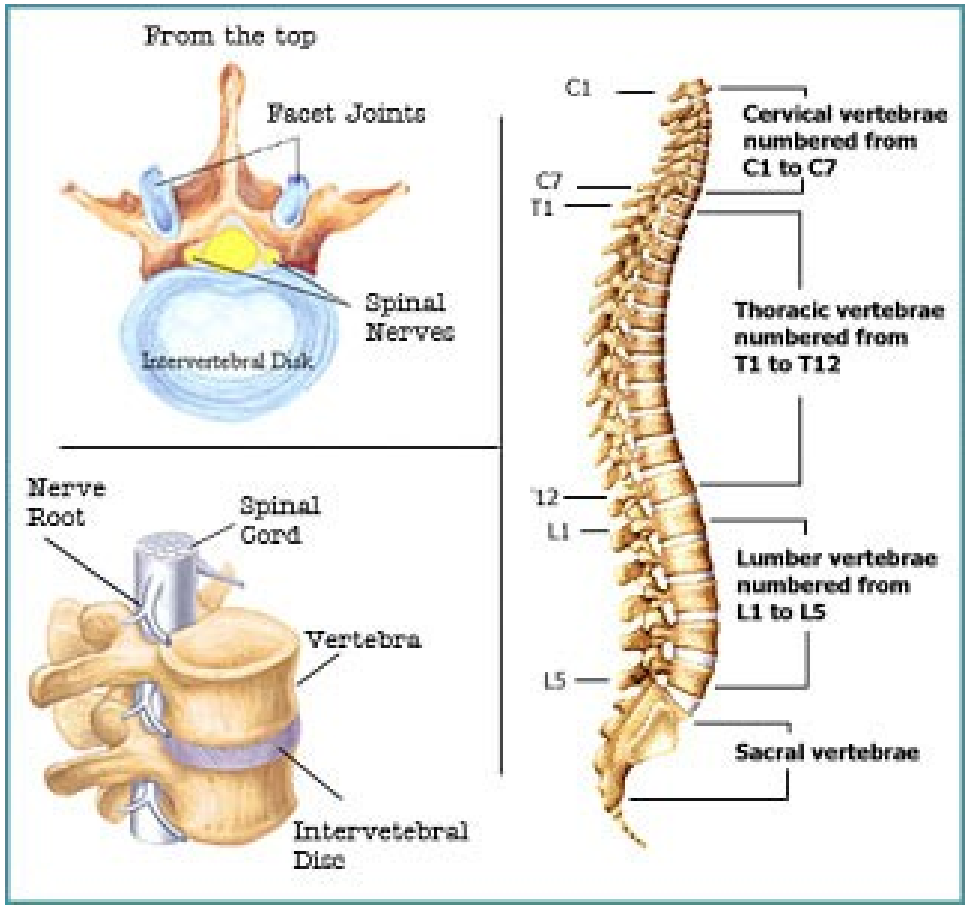

Figure 1- 1: Anatomy of the spine. Image - http://www.kinecare.net/treatments.html

The IVD is a highly specialized structure that enables motion of the spine and transmits mechanical load through the spinal column while providing a resistive force to keep the vertebrae apart during compression. 7-10 mm in diameter and approximately 4 cm in thickness around the lumbar region of the spine, the IVD is the largest avascular

tissue in the human body [75]. The percent composition of each region of the IVD varies with age and location within the spine but can be categorized into three distinct anatomical regions: Nucleus Pulposus (NP), Annulus Fibrosus (AF) and Cartilaginous End Plate (CEP) [Figure 1- 2, Figure 1- 3].

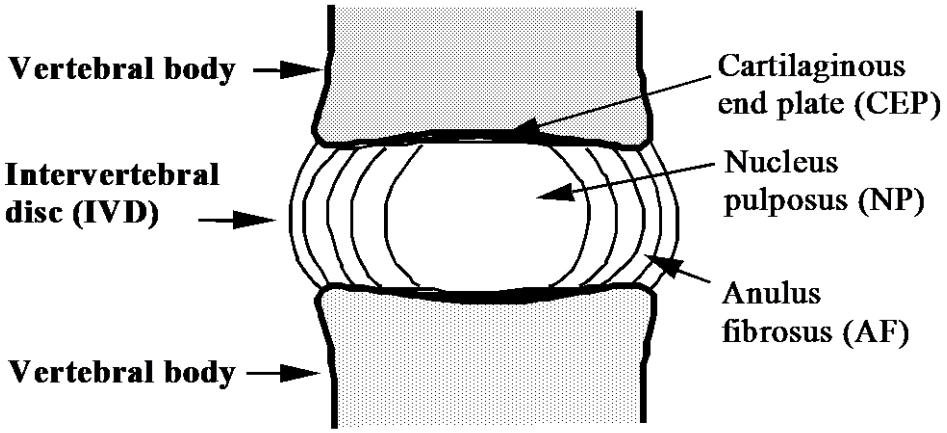

Figure 1- 2: Anatomy of the intervertebral disc.

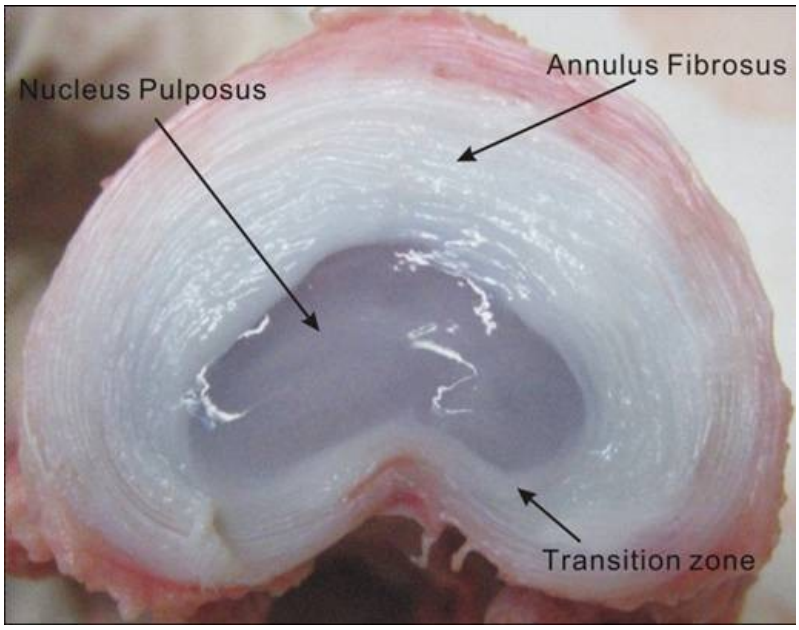

Figure 1- 3: Transverse view of a porcine lumbar disc.

NP tissue is confined to the center of the disc [Figure 1- 3]. It has a highly hydrated extracellular matrix primarily composed of type II collagen and aggrecan at a 1 to 20 ratio (1 to 2 in articular cartilage) [65]. The collagen fibers are randomly oriented within this matrix. Aggrecan is a highly negative and hydrophilic proteoglycan compound that is abundant in this fluid matrix plays a crucial role in NP tissue function. Its hydrophilic nature allows the disc to stay hydrated and confers a fluid pressure that prevents vertebrae from collapsing during compression [6]. The fluid like behavior of this matrix ensures that forces are evenly distributed to the surrounding AF region [80].

Surrounding the NP tissue on the perimeter is the highly organized, concentric lamellae of the AF tissue [Figure 1- 3] [60]. AF tissue is composed of collagen I fibers that are parallel within each lamella and approximately 60° to the vertical axis and alternate right and left in adjacent lamella [18]. AF restrains the swelling pressure of NP within the disc during compression and bears tensile and compressive loads during motion. In contrast to NP tissue, AF tissue display viscoelastic and anisotropic properties [80].

The CEP is a thin layer (approximately 1 mm in thickness) of hyaline cartilage that interfaces between the vertebral body and the IVD [Figure 1- 2]. This structure prevents NP leakage to the superior and inferior vertebral bodies and provides lateral support to IVD and vertebral bodies to prevent fracture during load transmission.

1.2: Cells from different regions of the IVD

Young IVD, or immature NP tissue, contain cells with spherical morphology and are thought to be of notochord origin. It has been reported that notochordal cells contain immature mitochondria associated with endoplasmic reticulum, and has glycogen deposits [25,84]. These cells, however, disappear with age and are replaced by a more chondrocyte-like cell type [67,85]. While the reason for the change in cell phenotype is still unclear, it may be a contributing factor to age dependent variation in disc mechanical properties and subsequently to disc degeneration. However, it has been reported that mature NP cells are more resistant to nutritional stress than notochordal cells [25]. Cell density within the NP tissue varies with region (highest at annulus edge where the nutrient supply is highest) and age but is approximated to 5,000 cells/mm^3 [62].

AF cells have a mesenchymal origin and an ellipsoidal morphology, where the long axis of the cells aligns with the orientation of the collagen fibers [67,80]. These cells are primarily composed of type I, II collagen and proteoglycan and therefore are considered similar in function to chondrocytes and fibroblasts. Cell density in the AF region is significantly higher compared to NP region approximating 7000 to 12000 cells/mm^3 [30,62]. As can be seen in Figure 1- 3, the AF and NP regions are integrated by a transition zone. As the cells approach the transition zone, morphology changes gradually from ellipsoidal to spherical suggesting the different mechanical properties of these cells and possibly their function within the tissue.

1.3: Nutrient supply to IVD

As previously mentioned, there is no direct blood supply in to the IVD. Blood vessels on the periphery of the IVD provide nutrients to the outer AF. Capillaries extend from the blood supply to vertebral bodies, but end without penetrating the CEP [Figure 1-4] [62,87]. As such, nutrient transport across the IVD is significantly affected by diffusivity and permeability of the tissue, concentration gradients that arise due to cellular consumption and coupling effects between nutrients and metabolites. Convective transport, which originates from fluid discharge of the disc under loading, is not considered to be a significant contributor to transport of small molecules such as glucose and oxygen. Thus, transport of nutrients and metabolites relies heavily on diffusion [87].

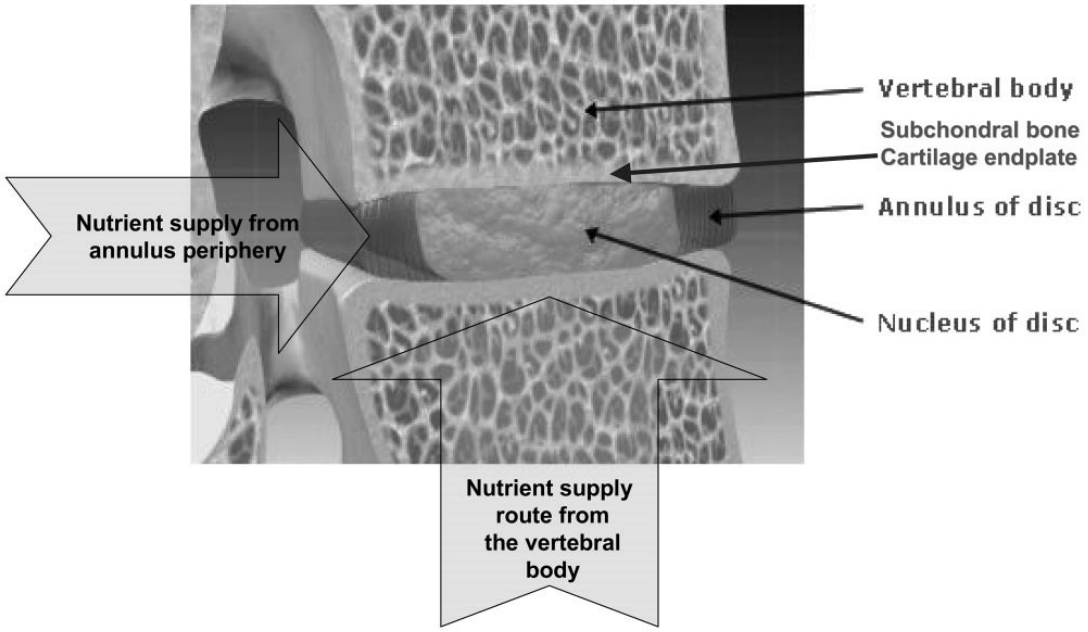

Figure 1- 4: Nutrient pathways to the IVD.
Image: Nutrition of the intervertebral disc, Urban et al.

Recent studies have shown that mechanical loading indirectly affects solute transport in cartilage-like tissue by changing the diffusivity of tissue [32,74]. For example, Yuan et al. demonstrated that oxygen diffusivity in bovine annulus fibrosus tissue was significantly decreased with increased compressive strain magnitude [91]. Similarly, Jackson et al. showed that increase in compressive strain, significantly decreased glucose diffusivity of IVD tissue [39]. Since nutrients must diffuse through vertebrae and CEP to reach IVD cells, sclerosis or hardening of the subchondral bone and calcification of the end plate significantly hinders the nutrient supply for these cells. Decrease in blood supply, which may occur due to diseases such as atherosclerosis of the abdominal aorta, sickle cell anemia, and Caisson disease also restricts proper nutrient supply to the disc.

1.4: Energy Metabolism of IVD

Adenosine tri-phosphate (ATP) is the primary energy currency for cellular activities. Although glucose is the most commonly used substrate for ATP production in eukaryotic cells, other sources such as fatty acids and amino acids can also be used as substrates. For example, because of high energy demands, heart muscles utilize fatty acids as their primary energy source resulting in high ATP yield. A simplified schematic of cell energy production in cells is depicted in Figure 1- 5. In effect, two processes contribute to ATP production: glycolysis and aerobic respiration.

As illustrated by Figure 1- 5, energy metabolism can be divided into five steps. Since energy metabolism occurs in the cytosol, the substrate must first be transported into

the cell. However, some cells including, immature NP cells and chondrocytes, have been reported to contain glycogen - glucose deposits [85]. When required, glycogen can be broken down to glucose and be utilized for ATP production. The process of breaking down glucose is known as 'glycolysis'. Pyruvate, an intermediate of glycolysis, may enter mitochondria to undergo aerobic respiration or, in the absence of sufficient oxygen may become lactate. Thus lactate can be used as a reference for glucose consumed for ATP production that does not undergo aerobic respiration. The net energy production of glycolysis via lactate is 2 ATP molecules per glucose molecule.

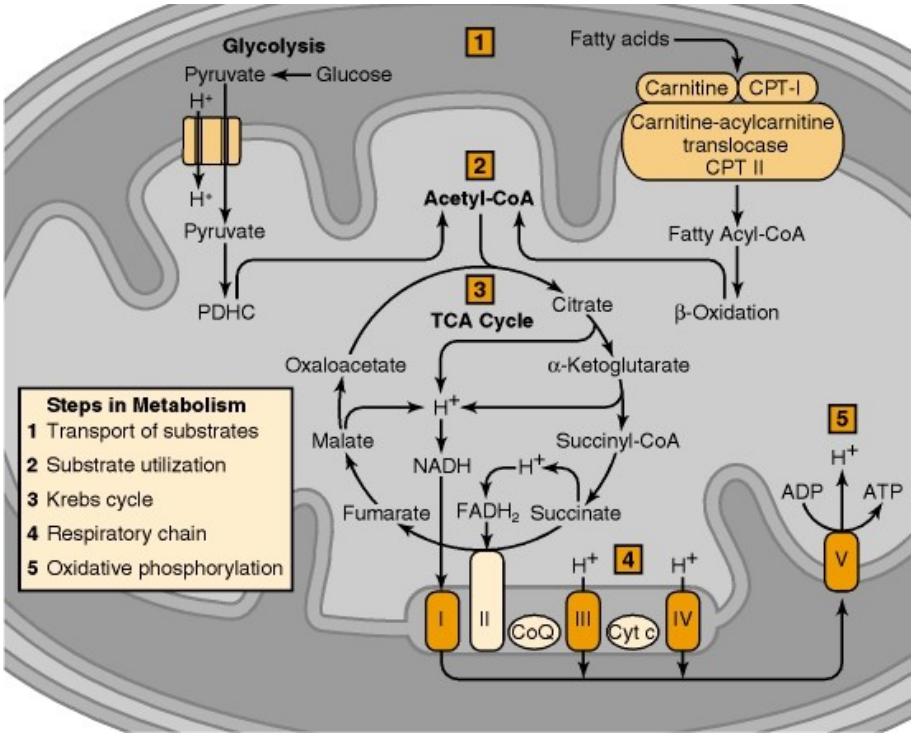

Figure 1- 5: Schematic representation of ATP production in cells.
Image: http://www.ncbi.nlm.nih.gov/bookshelf/br.fcgi?book=bnchm&part=A2959

Pyruvate (or other intermediates) that enters mitochondria is converted to Acetyle-coenzyme A, the starting compound for the Krebs cycle (also known as citric

acid cycle or tricarboxylic cycle – TCA). The Krebs cycle includes a series of chemical reactions which produces 2 ATP molecules per cycle and intermediates such as NADH, a compound necessary for oxidative phosphorylation (also known as the electron transport chain); a process that takes place in the inner membrane of the mitochondria. Five protein molecules (commonly known as subunit I through V) are required to stimulate and carry out ATP synthesis via electron transport. Nitric oxide (NO), a highly excitable molecule and a messenger for various cellular activities, is able to inhibit subunit IV (cytochome C oxidase) activity and as such is able to inhibit ATP synthesis via electron transport pathway. The theoretical net energy production of mitochondrial respiration is 36 ATP units per glucose molecule.

Like most cells, IVD cells use ATP as their primary energy form for cellular activities. A study conducted by Bibby and Urban demonstrated that IVD cell viability was more sensitive to glucose concentration and pH than to oxygen [5]. Although, studies have shown that NP cells are able to perform mitochondrial respiration, glucose consumption via lactic acid pathway was seen as the preferred method of ATP production at physiological conditions [5].

1.5: Degeneration of IVD

While the exact cause is unknown, five major factors may contribute to disc degeneration: 1) Nutrient supply, 2) Soluble regulators of cell function, 3) Genetic influences, 4) Ageing and senescence, and 5) Mechanical loading [4,6,18].

With an increase in disc degeneration seen in patients with atherosclerosis, sickell cell anemia, Caisson disease and Gaucher's disease, diseases which affect the nutrient

supply to the IVD, a prominent link between nutrient supply and disc degeneration has been suggested [18,46,47]. Recent studies show that alterations in cytokine such as IL-1 and TNF-α regulation can promote degenerative processes such as up-regulation of matrix degrading enzymes; abnormal synthesis of aggrecan, collagen I and II; angiogenesis; neuronogenesis; and cell death [18]. Twin-studies have illustrated that heritability of disc degeneration exceeds 60%, with genetic associations such as collagen IX and vitamin D receptor (VDR) polymorphism seen in a reasonable number of patients [3,18,79]. While physical stimulation is widely accepted as a regulating factor for proper cell function, studies show that abnormal over loading may cause injury to disc and induce degeneration [18,54,56,70].

The physiology and mechanical properties of the disc change with aging and disc degeneration. Primarily, the IVD loses its highly organized structure as the lamellae of the AF become irregular and gaps form within the NP. Aggrecan, generally a large molecule, degrade and become fragments of smaller molecules resulting in reduced disc hydration and swelling pressure. Due to this loss in swelling pressure, disc height is lost which in turn relaxes adjoining tissues and ligaments. *Ligamenta flava,* which connects adjacent vertebrae with each other, loses its tensile forces and elasticity as a result of this loss in disc height. It is believed that this causes the ligament to bulge into the spinal canal leading to spinal stenosis [75]. Also, the large, highly negative structure of aggrecan is thought to inhibit vascular and nerve in-growth and prevent or limit movement of large molecules such as cytokines and growth factors into the disc [44,61,77]. Therefore, decrease in aggrecan concentration may either induce or aggravate degenerative processes of the disc, and as such explain the increased

vasculature and nerve ingrowth seen in degenerated discs. Disc degeneration causes the composition of collagen to alter, with collagen fibers becoming denatured due to irregular enzyme activities. Increased amounts of fibronectin are seen in degenerated discs, confirming altered cellular biosynthesis [68]. Altered mechanical properties arising due to these degenerative changes to the disc may create abnormal stress distributions in AF, NP, and CEP regions, causing further injury to the disc and associated structures, thus catalyzing disc degeneration. Various spinal conditions associated with disc degeneration are shown in Figure 1- 6.

Figure 1- 6: Spine conditions. Image from http://www.laserspineinstitute.com/back_problems/

1.6: Discogenic back pain

Back-pain specifically arising from IVDs is termed discogenic back pain. Clinical studies show that patients with back pain due to IVD degeneration exhibit nerve ingrowth into discs (normally aneural and avascular), whereas patients with similar levels of disc degeneration and no complaints of back-pain do not exhibit nociceptive nerve ingrowth [18]. Studies are currently conducted to identify the processes that promote nerve ingrowth and their stimulants.

Angiogenesis (ingrowth of blood vessels) also occurs with disc degeneration possibly to compensate for the decreased nutrient supply to the disc under degenerative conditions. Studies have shown that vascular ingrowth may accompany nerve ingrowth to the disc and subsequently stimulate nociceptive nerve growth [71]. Aggrecan has been implicated in having inhibitory effects on nerve ingrowth. As disc becomes degenerated, aggrecan is degraded leading to a reduced inhibitory effect and consequently allowing nerve ingrowth [44].

1.7: Mechanotransduction

Cells within our body are constantly stimulated by changes in their environment. These could be biochemical stimulations arising from changes in various protein or ion concentrations, or physical stimulations from hydrostatic and osmotic pressures, compressive, tensile and shear stresses and strains and electro-kinetic forces. The magnitude and frequency of these forces are dependent on their environment and function. For example, articulating joints and ligaments are constantly exposed to static

and dynamic tensile and compressive loading. On the other hand, blood cells are constantly exposed to shear stresses associated with fluid flow. At a cellular level, these physical forces are translated as increased or decreased cell membrane tension and cell deformation. Cells respond to these stimuli by changing rate of cell division, differentiation, movement, signal transduction, gene expression, secretion, endocytosis and apoptosis [2,52]. The process of identifying a physical stimulation and translating it to an appropriate response is known as mechanotransduction.

Studies conducted on bone marrow derived mesenchymal stem cells have shown that mechanical loading is capable of directing differentiation of these stem cells toward chondrogenesis [33,34]. Numerous studies conducted on various cell types including chondrocytes and IVD cells have illustrated that mechanical loading is able to regulate the cellular biosynthesis, and may in fact be essential for maintaining normal phenotype of these cells [26,36,37,45,57,81]. Mechanical loading at non-physiological levels has been implicated as a contributing factor to alterations in tissue biomechanics and thus loss of proper function [28,89]. Therefore a need persists to identify how various mechanical forces are perceived by IVD cells and optimum mechanical stimulations that promote tissue regeneration and prevent or retard disc degeneration.

1.8: Nitric oxide

Nitric oxide (NO) is a potent inter- and intra cellular signaling molecule. Investigators have shown that, in certain cell types, NO can induce transient inhibition of mitochondrial respiration by reversibly binding to cytochrome c oxidase [8,9]. Various chondrocytes studies have also reported that NO inhibits proteoglycan synthesis [82] and

cell proliferation [7]. Further effects of NO include matrix breakdown activity, cell apoptosis and cytoskeleton reorganization. Studies have shown that herniated IVDs spontaneously secrete NO among other cytokines and as such NO might have a significant role in IVD tissue regulation and degeneration. We investigated NO production associated with mechanical loading to identify possible effects on mitochondrial respiration of IVD cells.

Chapter 2: OBJECTIVES OF STUDY

2.1: Significance of this study

As stated earlier, back pain is a significant socio-economic burden in our society affecting greater than 80% of the total population. While etiology of low back pain is still unknown, degeneration of the disc is a favored candidate [10]. Heritability, malnutrition and abnormal mechanical loading have been suggested as possible causes of disc degeneration. However, the exact pathways leading to disc degeneration remain unknown.

Functionality of the IVD is highly dependent on the proper maintenance of its extracellular matrix. Over time, this energy demanding process may be affected by poor nutrient supply to the disc, leading to insufficient energy metabolism and cellular biosynthesis. Previous studies have shown that extracellular ATP mediates matrix production under mechanical loading [13,64]. A study conducted on an osteoarthritis model showed that decrease in intracellular ATP promoted cartilage degeneration [42]. Similarly, ATP production and release may have a significant effect on proper maintenance of the IVD. To understand the effects of energy metabolism on the disc degeneration, we must first understand how energy metabolism is regulated under normal physiological conditions. Since the IVD is constantly subjected to mechanical loading, here we investigate the effects of mechanical loading on energy metabolism of IVDs at various physiological frequencies.

Knowledge gained from this study will help us understand how various mechanical forces are perceived by IVD cells and in particular identify their effect on cell

energy metabolism. Such information will facilitate the development of new clinical strategies to prevent or retard the degenerative processes of IVDs by promoting energy production and nutrient transport using different mechanical loading regimes.

2.2: Objectives

Mechanical loading of the spine compel fluid discharge from the disc to generate necessary resistive forces. As a direct result of decreased fluid level, nutrient supply to the cells decreases. Studies have shown that increase in compressive strain magnitude significantly decreased diffusivity and permeability of tissue thus affecting the nutrient supply to the cells [39,91]. Subsequent changes in tissue osmolarity and pH may also affect nutrient transport to the cells. Dynamic loading may also indirectly affect nutrient supply to the cells by altering solute transport in tissue [32]. Additionally, compressive and tensile forces transferred to IVD cells via the extracellular matrix of the disc can directly induce cell deformation which may trigger cellular responses such as change in cell membrane properties and ATP release. However, since the mechanical forces on the IVD are translated to cells via its dense matrix, cells in different regions might respond differently to the same stimuli [80].

In this study, cells were isolated from their surrounding matrix in order to identify how mechanical loading intrinsically affect cell energy metabolism. The objectives of this study were to investigate:

1) The effects of static loading on IVD cell energy production;
2) The effects of dynamic loading on IVD cell energy production;
3) Differences in response to mechanical stimulation between AF and NP cell.

Chapter 3: MATERIAL AND METHODS

3.1: Cell Isolation

IVD tissues from 2-3 month old pigs, weighing approximately 200-250 lbs. were used for this experiment. The pigs were obtained from a local slaughter house and dissected approximately within 2 h of sacrifice.

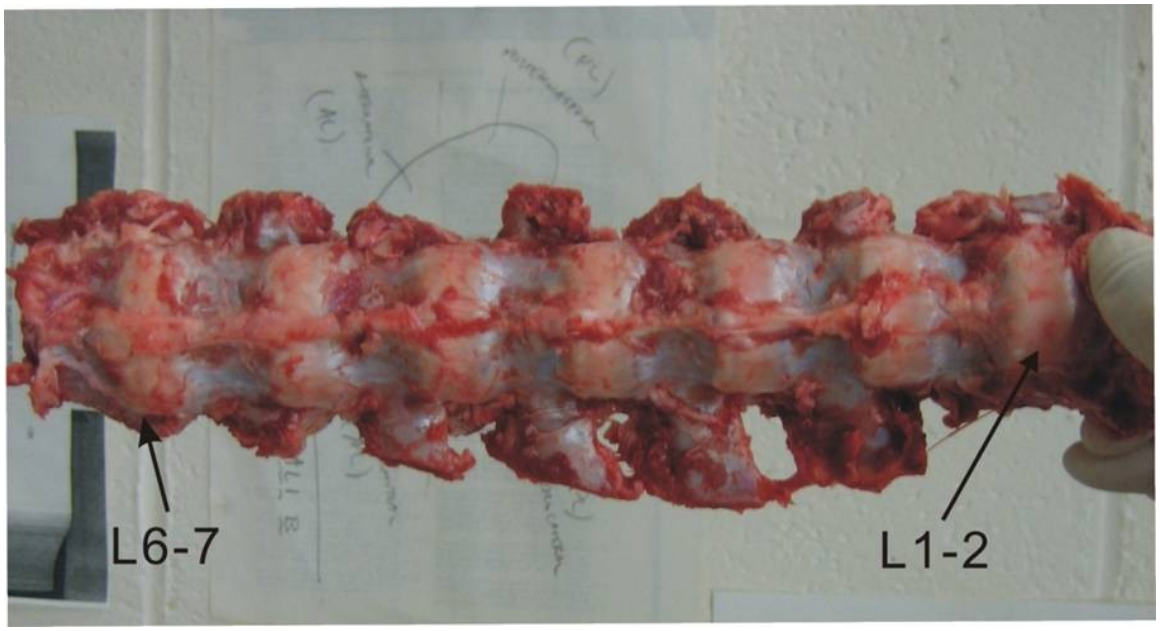

Figure 3- 1: Porcine spine.

The spines were extracted using an electric saw and bone cutting forceps [Figure 3- 1]. After careful removal of excess tissue, the spines were rinsed with sterile phosphate-buffered saline (PBS) containing 10% antibiotic-antimycotic (Invitrogen Corp.) 3 to 4 times. Spines were then moved to a biological safety cabinet and sprayed with 70% isopropyl alcohol to minimize contamination. To open each disc, first, a surgical blade was inserted at the center of IVD from outer AF to the center of NP region. Then a circular transverse cut was made to minimize AF and NP tissue mixing.

Following the opening of the disc, outer AF tissue and NP tissue were extracted independently using a surgical scalp and tweezers and placed in enzyme solution. The AF tissue was chopped finely to enhance tissue digestion. The enzyme solutions were made of Dulbecco's Modified Eagle Medium (DMEM, Invitrogen Corp.) supplemented with 15% fetal bovine serum (FBS; Invitrogen Corp.) and 1% antibiotic-antimycotic. For AF tissue, digestion solution was supplemented with 1.5 mg/mL collagenase type II (Worthington Biochemical Corp., Lakewood, NJ), and protease (Sigma Aldrich) 0.6 mg/mL. NP tissue digestion solution was supplemented with an equal concentration of protease but with slightly less collagenase type II concentration, 0.75 mg/mL. The tissue samples were kept on a plate shaker overnight at 37°C, 5% CO_2 and 21% O_2 tissue culture incubator [59].

Following tissue digestion, cell containing media were filtered with a 70 μm cell strainer (BD Biosciences, San Jose, CA) to isolate cells. Cells were then collected by centrifugation (NP: 1000 rpm for 4 min; AF: 2467 rpm for 10 min) and re-suspended in 10% FBS, 1% antibiotic-antimycotic DMEM.

Previous studies have observed changes in IVD cell phenotype due to sub-culturing [11]. To eliminate these phenotypic changes, fresh porcine cells were utilized in this study.

3.2: Agarose disc sample preparation

Number of cells obtained from tissue was calculated using a hematocytometer (Hausser Scientific, Horsham, PA). Cells were then suspended in DMEM (10% FBS, 1% antibiotic-antimycotic) at ten million cells per mL cell density.

4% low-melting agarose (Sigma Aldrich) solution was made with phosphate-buffered saline and sterilized using an autoclave machine. This solution was then mixed at a 1:1 ratio with cells to obtain final cell density of five million cells per mL in 2% agarose. The cell-agarose mix was poured on to a custom made Teflon mold to obtain discs with 8 mm in diameter and 1 mm in thickness [Figure 3- 2]. Once the discs solidified, they were transferred to Petri dishes containing DMEM supplemented with 10% FBS and 1% antibiotic-antimycotic and cultured overnight in a cell culture incubator prior to conducting experiments.

Previous research has shown that three-dimensional agarose culture is able to retain IVD cell phenotype [21,22]. Additionally, theoretical studies have demonstrated that 2% agarose exhibits isotropic properties and have minimal effect on transport of small solutes [23,24]. Thus variations in energy metabolism due to nutrient transport are eliminated in this study. Also, we believe at the given dimensions of the agarose disk, it is able to produce uniform force distribution to all cells within construct [63].

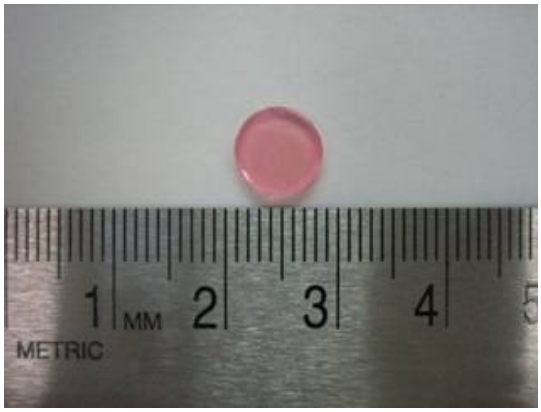

Figure 3- 2: 2% agarose disc. The disc is 8 mm in diameter and 1 mm in thickness. Cells were seeded at 5,000,000 cells per mL cell density with each sample containing 500,000 cells.

3.3: Bioreactor

Custom designed bioreactor system [Figure 3- 5: Bioreactor system.] used in this experiment is introduced in detail by its designer [Jessica Czamanski, Masters Thesis, Dept. of Biomedical Engineering, University of Miami]. Brief introduction to the main components of the system is given here. An eccentric cam follower system was used to generate sinusoidal displacement. The cam [Figure 3-5 (a)] movement was governed by a stepping motor. This cyclic displacement is passed to the shaft [Figure 3-5 (d)] and then to the compression plate [Figure 3-5 (h)] via the follower [Figure 3-5 (b)] sitting tangent (directly below) to the cam.

Dynamic loading frequency was varied by changing applicable parameters in the interface program (LABVIEW). Changes to strain level was manually adjusted and verified by LVDT measurements [Figure 3-5 (e)]. Given the minute change in displacement (200-500 μm), reference points slightly further from the center were utilized for this adjustment.

Samples were placed on a porous filter **[**Figure 3- 3**]** inside the chamber **[**Figure 3-4] with predefined amount of culture media. Porous filter enables nutrient supply to the bottom surface of the cell-agarose disc. Compression plugs were initially set to rest on the samples and locked in place by lowering a nut [Figure 3-5 (j)] to prevent unintended compression of samples during experiment set-up. The position of the cam was set to neutral position (displacement at zero) prior to inserting samples. After the compression samples were kept in position, the compression plate [Figure 3-5 (h)] was lowered through the rods and tightly fitted using nuts. At this point in time, the locks placed to prevent samples from unintended compression were released. To obtain 5% preloading

(offset), a 0.001 inch think shim (Small Parts Inc.) was folded four times (total thickness 0.004 inch / 100 μm) and inserted between the cam and the follower [Figure 3-5 (c)]. Bioreactor system was then transferred to a tissue culture incubator for the duration of the experiment. At the completion of each experiment, the nuts intended to safeguard samples were returned to locking position prior to releasing the compression plate and removing samples.

Chambers, porous filters and plugs were sterilized using standard autoclaving procedures in-between experiments.

Figure 3- 3: Porous filter. The filter is 12.7 mm is diameter and is made of stainless steel. Pore size is 20 μm and was 40% porosity.

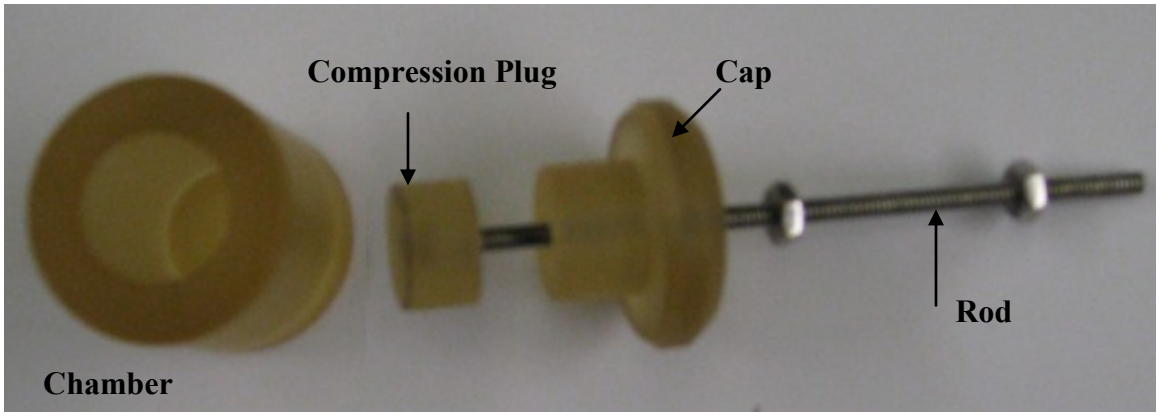

Figure 3- 4: Chamber and compression plug. Each chamber contained one sample that was either compressed or was used as a control. Samples were compressed by the movement of the compression plug. Movement of the compression plug was guided by the rod. Chamers were closed by a cap. Chamber, cap and plug were made from an autoclavable polymer. Rods were made of stainless steel.

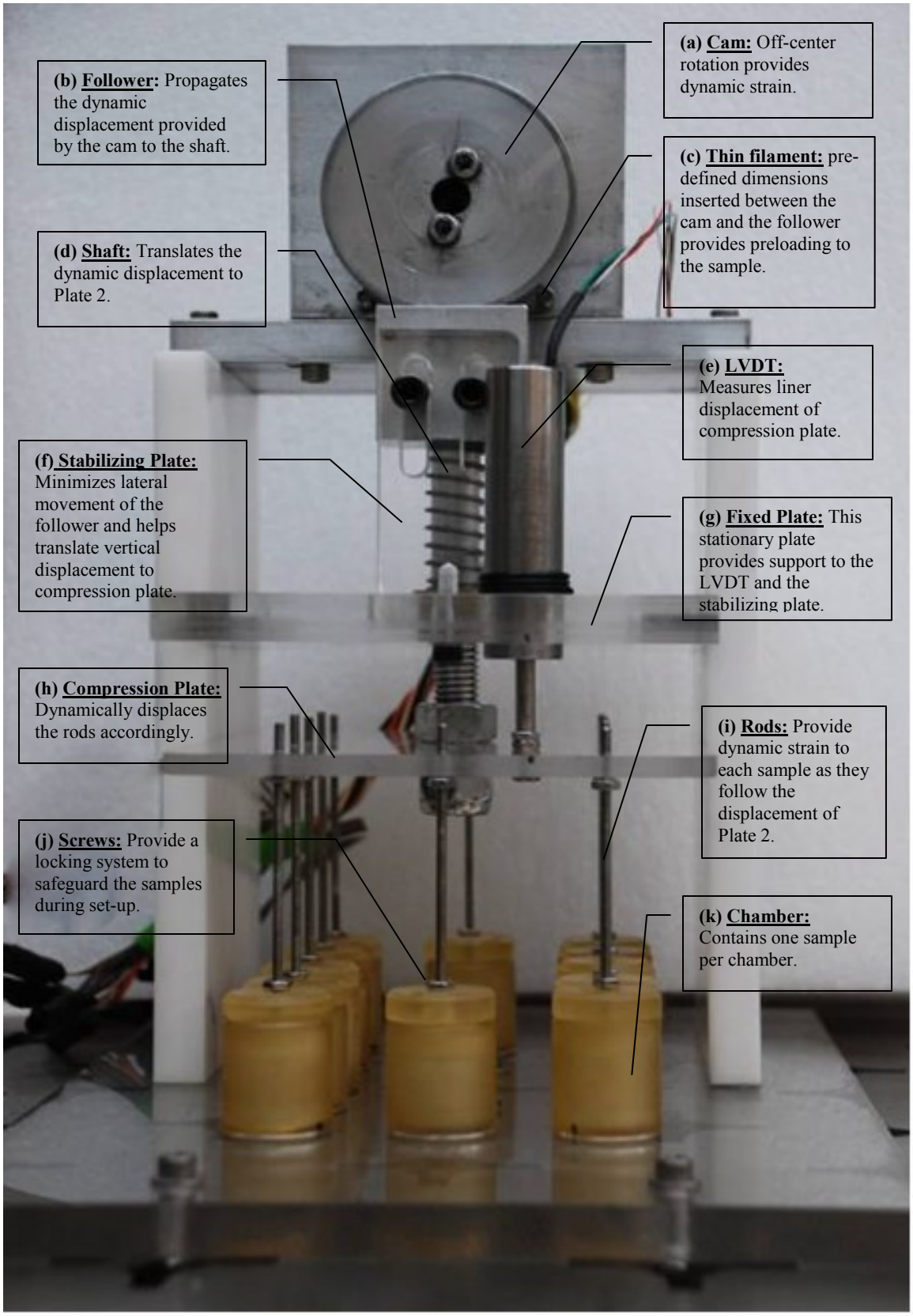

Figure 3- 5: Bioreactor system.

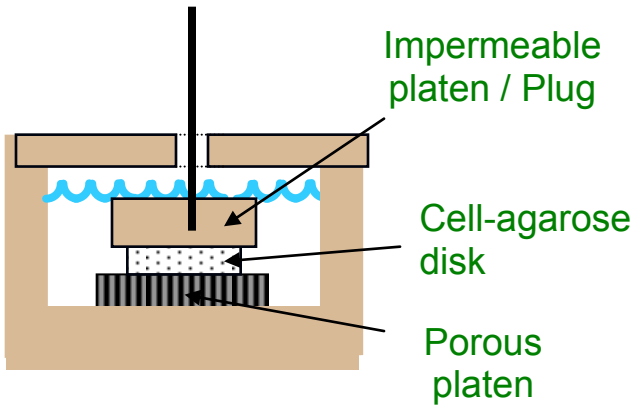

Figure 3- 6: Sample setup. A porous filter was placed at the bottom of each chamber. Cell-agarose construct was placed on top of this porous filter. This porous filter enables nutrient supply to the cells at the bottom of the sample. A plug, made from the same material as chamber, was used to compress the sample. The movement of the plug was governed by the rod attached to the plug. A plug was placed on the control sample but this plug was not subjected to any compression.

3.4: Experiment protocol

All samples were cultured in DMEM supplemented with 10% FBS and 1% antibiotic-antimycotic for a minimum of 12 h (up to 70 h) prior to conducting loading experiments. Due to interference of FBS in certain chemical assays, all samples were rinsed in DMEM without any supplements immediately before each experiment.

Each sample was placed in custom made chamber on top of a porous filter. 600 µL of DMEM (without any supplements) was added to each chamber. For control samples, a plug, without any loading, was set to rest on top of the samples **[**Figure 3- 6**].** We believe this control set up is subjected to similar nutrient supply as the compressed samples, thus eliminates the differences in energy metabolism due to a change in nutrient supply. Compression samples were loaded to the bioreactor as mentioned in the previous

section. The bioreactor system and control samples were kept in a tissue culture incubator at 37°C and 5% CO_2 for the duration of the experiment.

The experimental categories can be divided as follows: Control group, kept at same culture conditions without subjecting to mechanical loading. Static compression group – samples subjected to either 15% or 30% static compression for 4 hrs [Figure 3-7]. Dynamic loading group – samples subjected to dynamic loading frequencies at 0.1 Hz, 1 Hz and 2 Hz for 4 hrs at 15% total strain (5% preloading and 10% dynamic) [Figure 3- 8].

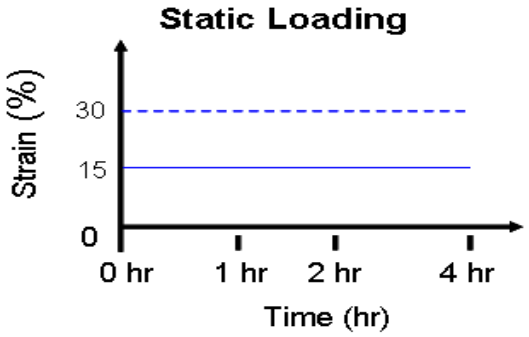

Figure 3- 7: Graphical representation of static loading experimental protocol. All samples were subjected to either 15% or 30% static strain for 4 hr.

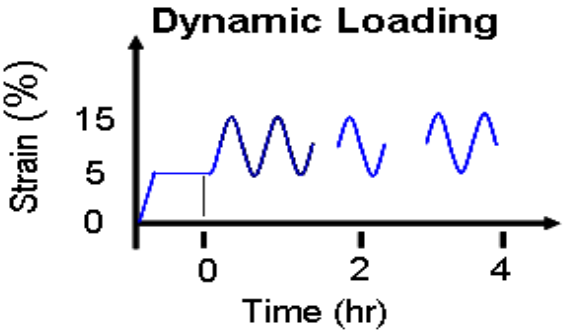

Figure 3- 8: Graphical representation of dynamic loading experimental protocol. All samples were initially set to 5% strain or preloading (offset) followed by 10% dynamic strain for 4 hr.

At the end of each experiment, cell-agarose discs were collected from each chamber into separate sterile Eppendorf tubes. 30 μL of culture medium was mixed at a 1:1 ratio with ATP stabilizing solution (3mM EDTA) and boiled for 2 min to preserve ATP released to culture media. The remaining culture media was collected without further processing and all samples were stored at -80°C until analysis.

3.5: Cell-agarose breakdown

Cell-agarose discs were defrosted and separated into halves using a pill-cutter. One half was placed in 500 μL of lysis buffer to break down agarose and release cells seeded within the construct. The lysis buffer was made by dissolving the following chemicals at given concentrations in sterile water: 15% 1.5 M NaCl, 15% 50 mM EDTA, 1% Triton-X 100 and 10% 100 mM TRIS-Cl at pH 7.4. The remaining half-disc was combined with another half-disc of the same experimental group for RNA extraction.

Cell-agarose constructs were broken down by utilizing homogenizing pestles and vortexing. These samples were heated at 65°C for 10 min before vortexing again to promote breakdown of agarose and cell release. Samples were heated for an additional 10 min at 65°C and then centrifuged at 9000 rpm for 10 min. The supernatant was collected and frozen at -80°C until measurements.

3.6: Chemical Assays

ATP assay Intracellular ATP and ATP released to media were measured using the Luciferin-luciferase method (Sigma). For intracellular ATP measurements, standard concentrations were made using lysis buffer used for cell-agarose breakdown. DMEM without supplements were used to prepare standards to measure ATP concentrations in media. When necessary, intracellular ATP and extracellular ATP samples were diluted in lysis buffer or DMEM without supplements respectively to bring measurements within the range of the standard curve. Final concentrations of samples were calculated based on linear curve derived from standard concentrations. These sample concentrations were converted to total amount of ATP based on sample volume and were then normalized to amount DNA content per sample to account for cell number variation.

Lactate assay Lactate concentrations in media were measured using L-lactic dehydrogenase enzymatic assay (Sigma). Standard curve for this assay was made using DMEM without supplements. If necessary, samples were diluted in DMEM without supplements to bring measurements within the range of the standard curve. Final concentrations were calculated based on a 2^{nd} order polynomial curve obtained from standard concentrations. These sample concentrations were converted to total amount of lactate per sample based on sample volume and were then normalized to amount DNA content to account for possible variations in cell concentrations.

NO assay NO production was evaluated by measuring nitrite concentration, a stable breakdown product of NO, using Greiss assay [20]. Standards were made with DMEM without supplements and the final concentrations were calculated using a linear curve

derived from standards. Similar to ATP and lactate productions, sample concentrations were converted to total amount of nitrite based on sample volume and were then normalized to amount DNA content per sample to account for possible variations in cell concentrations.

Glucose consumption measurements Glucose concentrations were measured at Diabetes Research Institute (DRI), Miami FL (Cobas C system, Roche). Culture medium from each sample was analyzed for glucose concentrations (C_final). DMEM without any supplements was used as the reference glucose concentration (C_0). The difference in concentrations (C_0 – C_final) provided the change in glucose concentration due to cellular glucose consumption. Total amount of glucose consumed was calculated based on sample volume and then normalized to the number of cells per sample by dividing it by respective DNA content per sample. Thus the results presented are the total amount of glucose consumed during the total length of the experiment normalized to the amount of cells.

DNA measurements DNA content of each sample was measured using a fluorometric assay (Quant-it, Invitrogen). DNA content of each sample was converted to DNA content per sample based on sample volume.

Biochemical assay data normalization As mentioned in each assay protocol, all measurements were normalized to DNA content per sample to account for variations in cell number. To evaluate the effects of compressions, the compressed sample values were normalized to respective uncompressed sample values. To analyze differences

between AF and NP cell types, values of NP cells were normalized to respective value (culture condition and assay) of AF cells.

Gene expression analysis Each sample contained approximately 500,000 cells. RNA from samples was extracted using Trizol (TRI reagent RT, Molecular Research Center, Cincinnati OH) and chloroform (Sigma). Sequential centrifugation in Iso-proponol and 75% ethanol at 12,000 rpm for 30mins was used to precipitate RNA in each sample. RNA concentrations and purity was spectrophotometrically evaluated (SmartSpec Plus Spectrophotometer, BioRad Hercules, CA). Reverse transcription to cDNA was performed using qScript cDNA synthesis kit (Quanta Biosciences, Gaithersburg, MD), 5 min at 22 ºC, and 30 min at 42 º C and 5 min at 85 º C.

Real-Time polymerase chain reaction method was utilized to measure relative mRNA quantities of the following genes: type II collagen, aggrecan and inducible nitric oxide synthase (iNOS). 18s was used as an internal control for each cDNA sample. Primer sequences used are given in Table 1: Primer sequences. δδCt method was used to calculate relative mRNA quantities [55].

Table 1: Primer sequences.

Gene			Sequence	Size	Gene Bank
Collagen II	sense		5'-TGAGAGGTCTTCCTGGCAAA-3'	163 bp	AF201724
	antisense		5'-ATCACCTGGTTTCCCACCTT-3'		
Aggrecan	sense		5'-AGACAGTGACCTGGCCTGAC-3'	151 bp	AF201722
	antisense		5'-CCAGGGGCAAATGTAAAGG3'		
iNOS	sense		5'-TGTTCAGCTGTGCCTTCAAC-3'	226 bp	NM_001143690
	antisense		5'-CAGAACTGGGGGTACATGCT-3'		
18s	sense		5-CGGCTACCACATCCAAGGA-3	188 bp	NR_002170.3
	antisense		5-AGCTGGAATTACCGCGGCT-3		

3.7: Statistical analysis

One way ANOVA analyses with post-hoc Student-Newman-Keuls test was performed using SPSS software (Chicago, IL) for multiple group comparison. Samples subjected to static compression and dynamic compression was analyzed separately. Unpaired student's t-test was perform using excel data analysis tool (Microsoft, Seattle, WA) for comparison between cell types. In all cases $p \leq 0.05$ was considered significant.

Chapter 4: RESULTS

Effects of static and dynamic mechanical loading on energy metabolism of IVD cells were evaluated in this study. A comparison was also made between AF and NP cells to identify differential response based on cell type. Results are statistically significant ($p<0.05$) unless otherwise stated. There were total of 15 samples per experiment per cell type.

4.1.1: Effects of Static compression on AF cells

ATP release from AF cells was not significantly altered by static compression of either strain level [Figure 4- 1]. Compared to control, AF cells subjected to 15% static compression displayed a significant increase in total ATP content [**Figure 4- 2**] ($p < 0.05$) and lactate production [Figure 4- 3] ($p < 0.05$). Though an increase is seen in glucose consumption at this static strain magnitude, it was not statistically significant [Figure 4- 4]. No significant differences relative to control were found in NO production [Figure 4- 5] due to 15% static compression.

Samples subjected to 30% static compression exhibited significant increases in glucose consumption [Figure 4- 4] ($p < 0.001$) and total ATP content [**Figure 4- 2**] ($p < 0.05$) relative to control. Additionally, there were no significant differences in lactate production [Figure 4- 3], NO production [Figure 4- 5] or ATP release [Figure 4- 1] due to 30% static compression. There was a statistically significant decrease in lactate production and a significant increase in glucose consumption due to increase in strain level from 15% to 30%.

No significant differences were observed in mRNA levels for aggrecan, type II collagen or iNOS [Figure **4- 6**] due to static compression of AF cells.

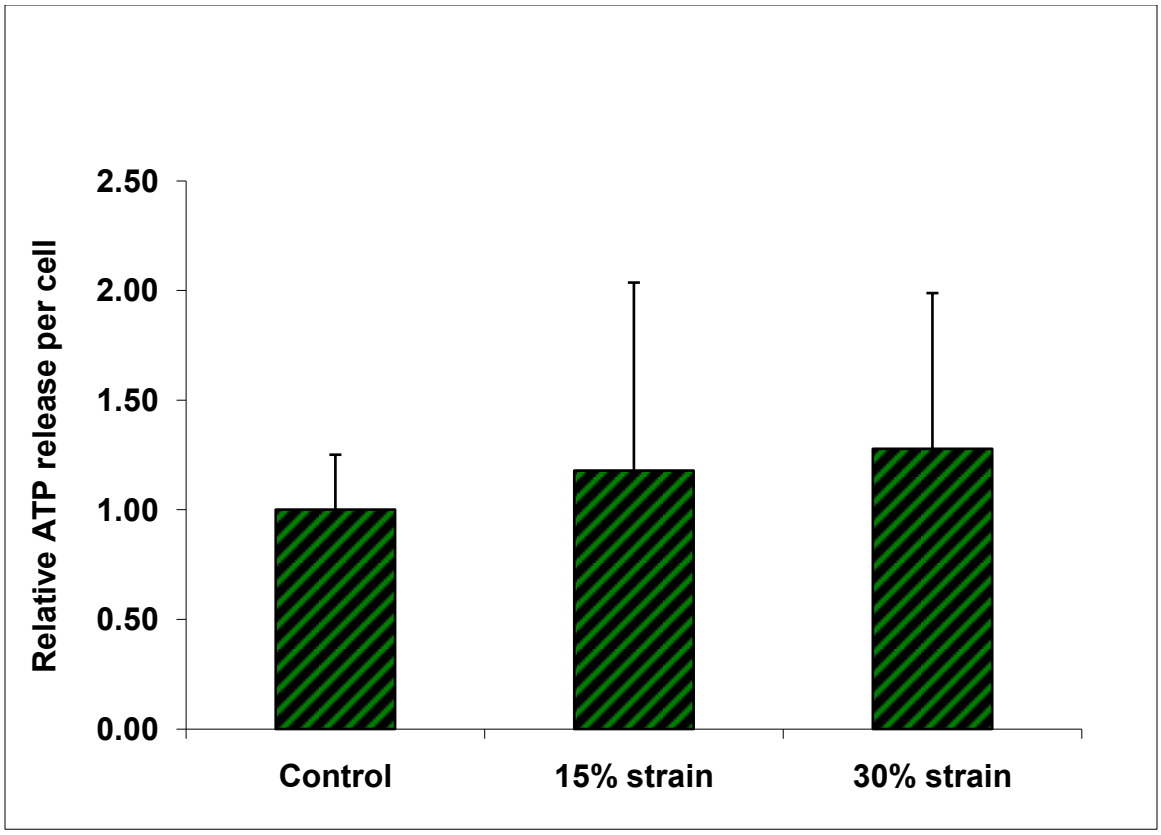

Figure 4- 1: Effects of static compression on ATP release from AF cells. This graph demonstrates the fold change in ATP release from AF cells due to 15% and 30% static compression. Although the data suggests an increase in ATP release due to static compression, this increase was not statistically significant. All data were normalized to total DNA per sample to account for variation in cell count.

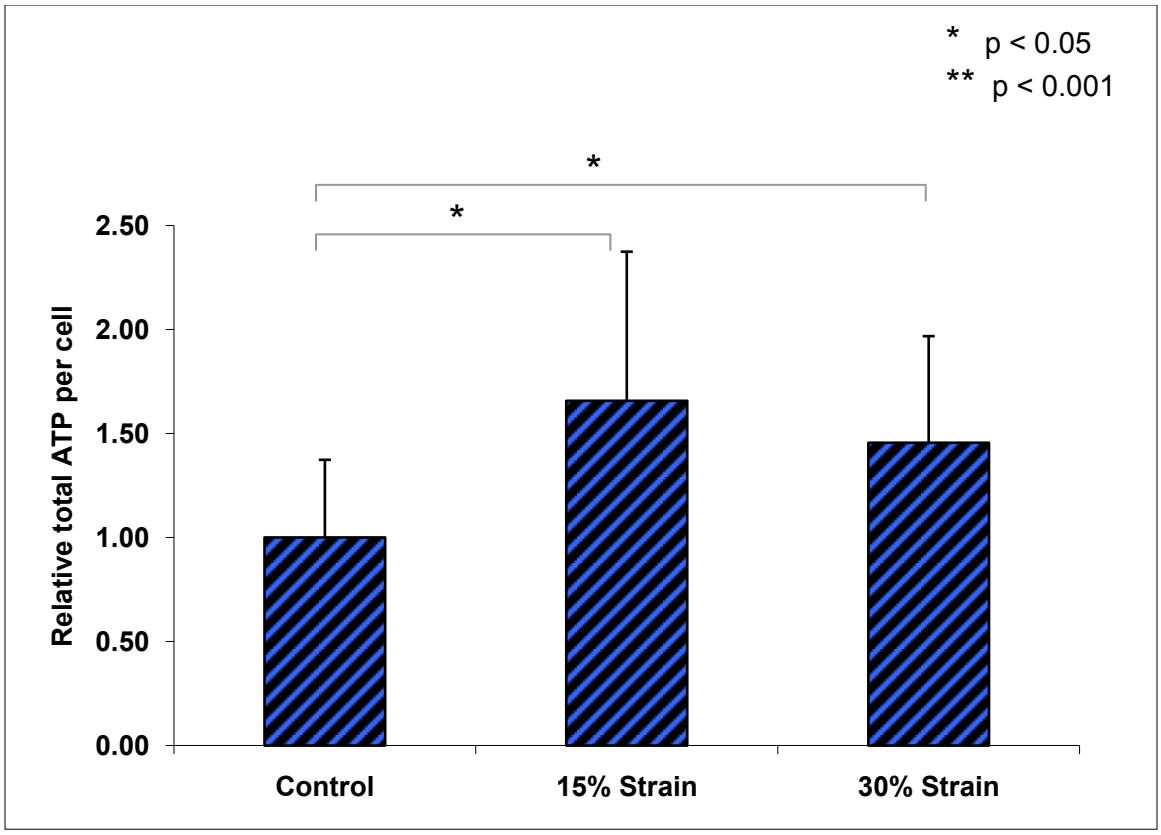

Figure 4- 2: Effects of static compression on total ATP of AF cells. This graph demonstrates the fold change in total ATP with respect to control samples following 15% and 30% static compression of AF cells. Total ATP content was significantly increased by both strain magnitudes ($p < 0.05$) however there were no significant differences in total ATP between 15% and 30% strain levels. All data were normalized to total DNA per sample to account for variation in cell count.

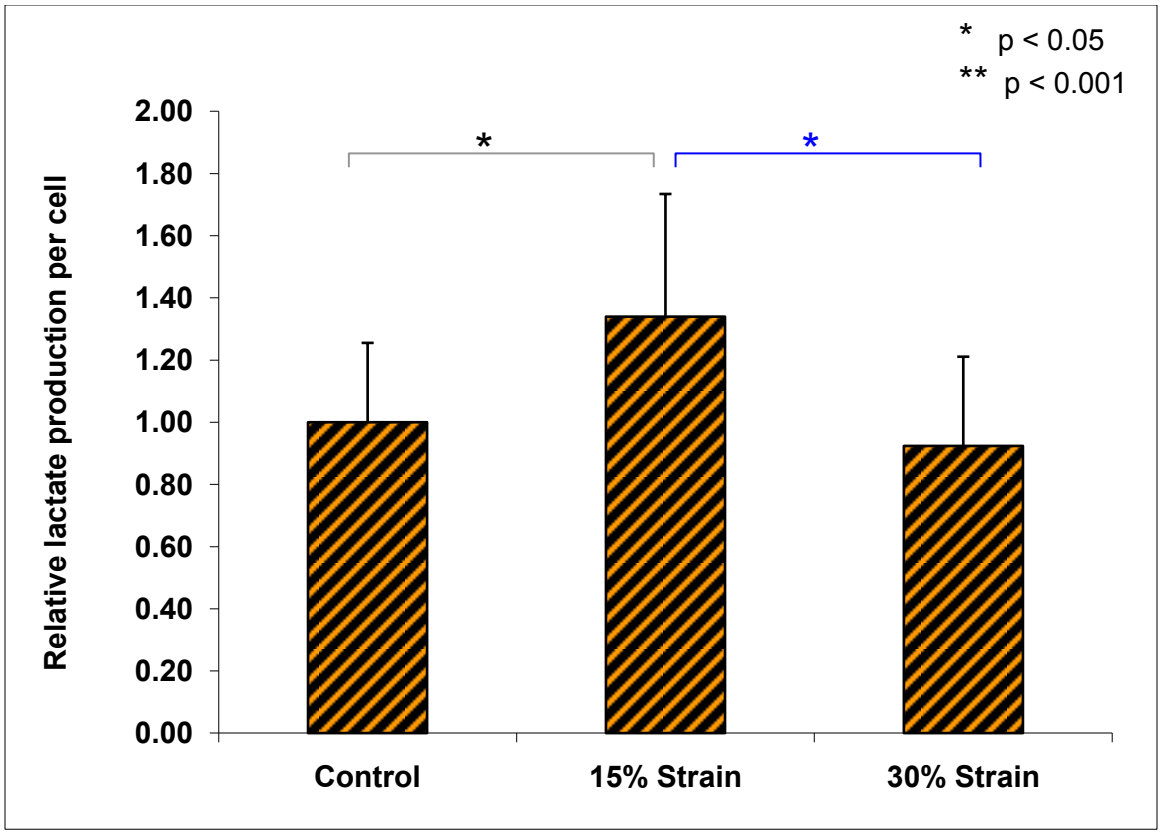

Figure 4- 3: Effects of static compression on lactate production of AF cells. This graph demonstrates the fold change in lactate production of AF cells relative to uncompressed samples due to static compression at 15% and 30% strain magnitudes. 15% static compression increased lactate production significantly with respect to control ($p < 0.05$) but there were no significant differences between uncompressed samples and samples compressed at 30% strain magnitude. There was a significant decrease in lactate production of AF cells when the strain magnitude was increased from 15% to 30% strain. All data were normalized to total DNA per sample to account for variation in cell count.

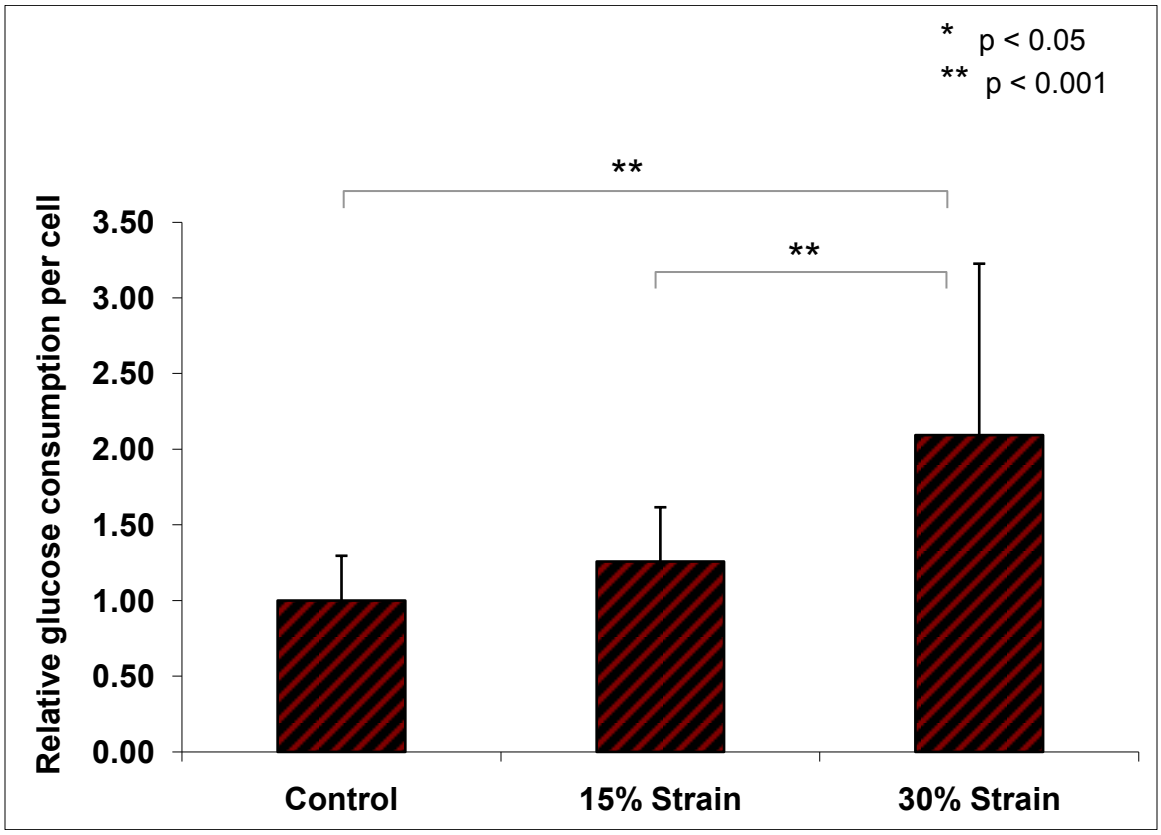

Figure 4- 4: Effects of static compression on glucose consumption of AF cells. Total glucose consumption was calculated based on the change in glucose concentration over the duration of the experiment and was normalized to DNA content per sample. Glucose consumption following 30% static compression was significantly higher with respect to uncompressed samples and samples compressed at 15% strain magnitude ($p < 0.001$). There were no significant differences in glucose consumption between uncompressed samples and samples compressed at 15% strain magnitude.

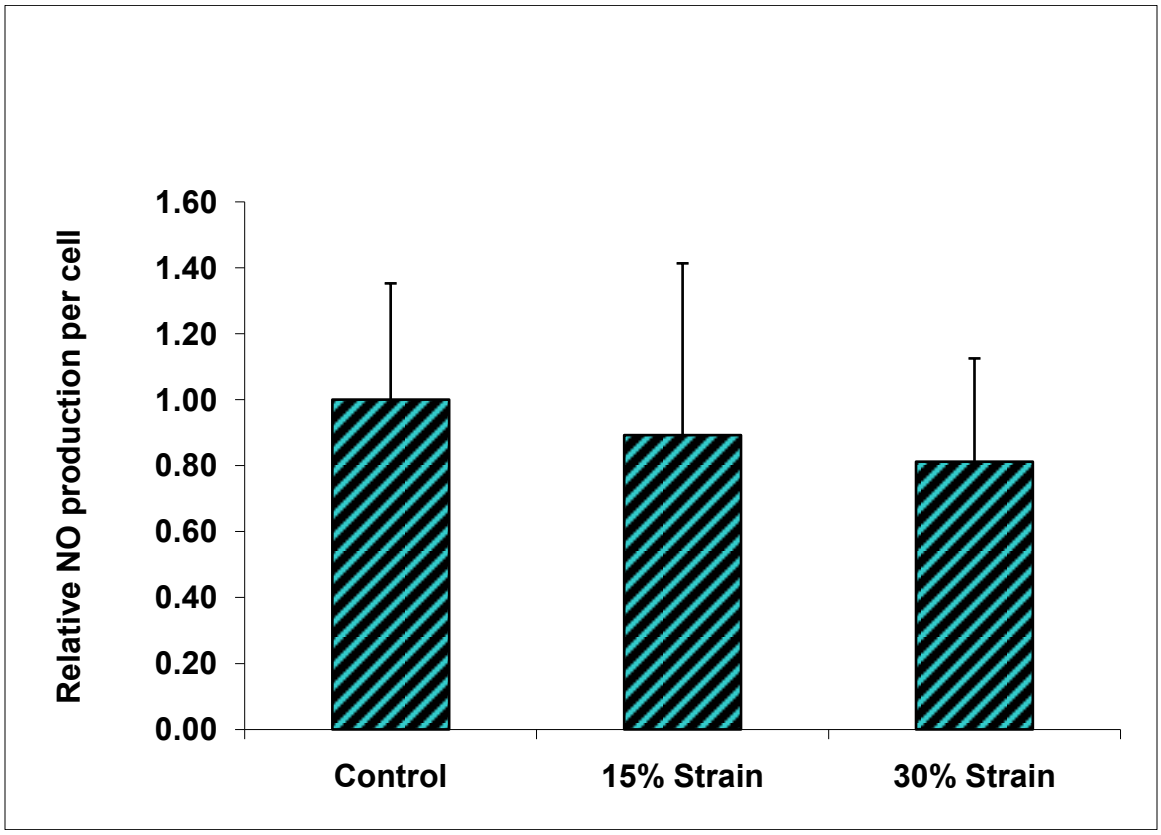

Figure 4- 5: Effects of static compression on NO production of AF cells. This graph depicts the fold change in NO production of AF cells due to 15% and 30% static compression with respect to uncompressed samples. The decrease seen in NO production under increased static strain magnitude was not statistically significant. All data were normalized to total DNA per sample to account for variation in cell count.

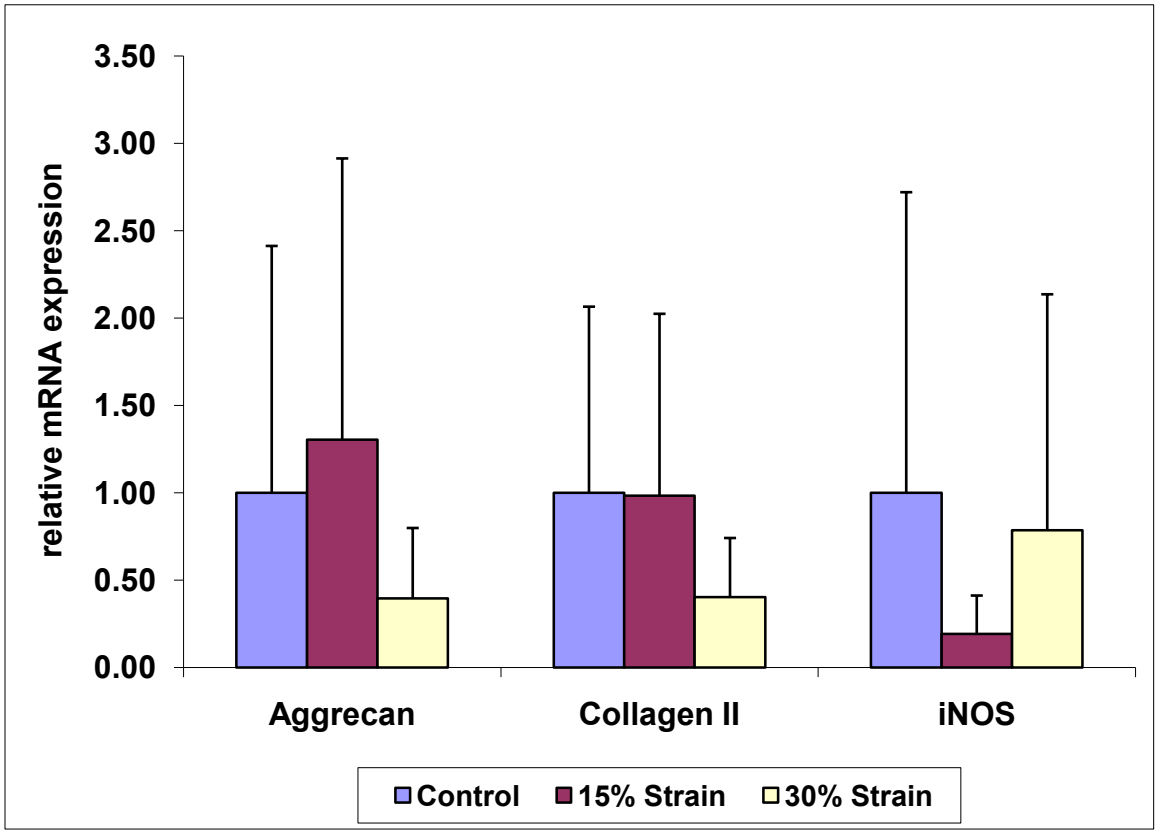

Figure 4- 6: Effects of static compression of extracellular matrix genes of AF cells. All cDNA samples were normalized to 18s internal control and then to respective control samples. Due to significant standard deviation, no significant differences were observed in relative gene expressions.

4.1.2: Effects of dynamic compression on AF Cells

ATP release was significant increased by 1 Hz and 2 Hz dynamic loading [Figure 4- 7]. All tested dynamic frequencies promoted total ATP content [Figure 4- 8] ($p < 0.05$), lactate production [Figure 4- 9] ($p < 0.05$), and glucose consumption [Figure 4- 10] ($p < 0.05$) relative to control. NO production was significantly increased by dynamic loading at the higher frequency levels (1 Hz and 2 Hz) but not at 0.1 Hz ($p < 0.05$) [**Figure 4- 11**].

Frequency dependence was not seen throughout AF dynamic loading groups except in NO production. There was a significant increase in NO production at 1 Hz and 2 Hz respect to 0.1 Hz [**Figure 4- 11**].

Dynamic compression of AF cells did not produce a significant variation in mRNA levels of aggrecan, type II collagen and iNOS [**Figure 4- 12**].

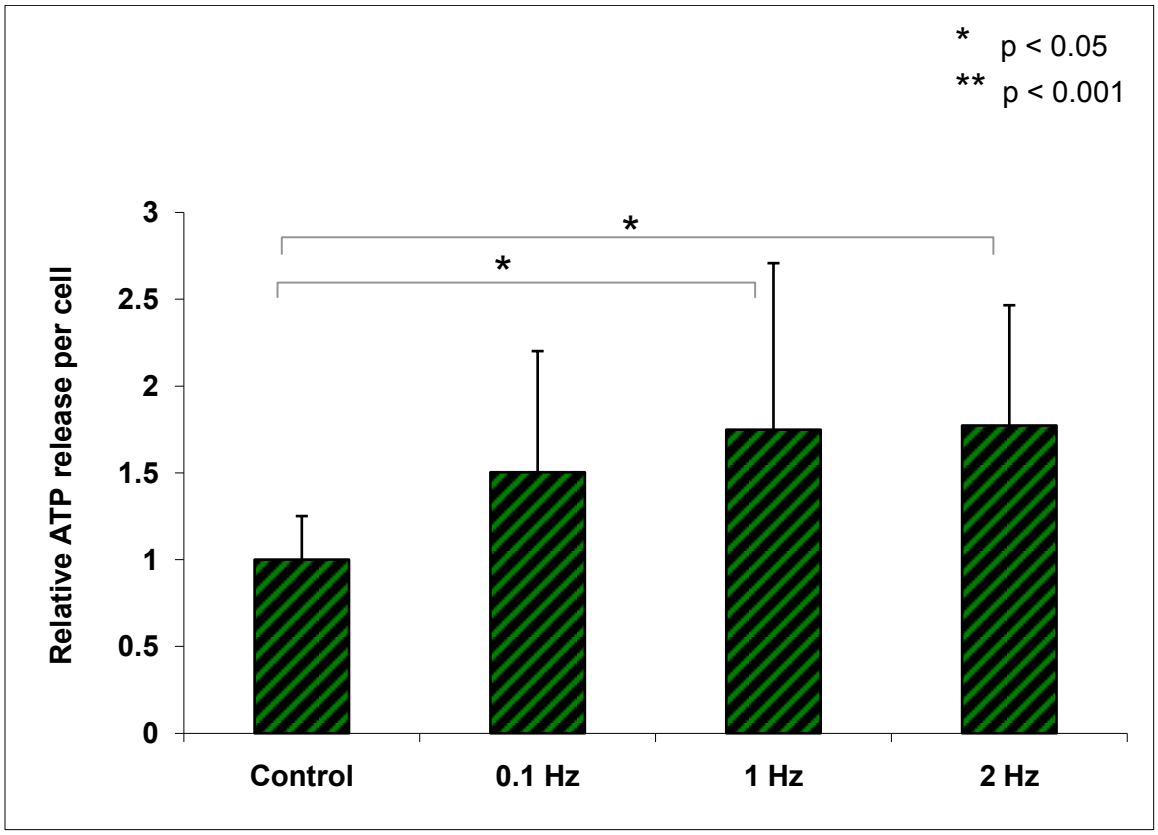

Figure 4- 7: Effects of dynamic compression on ATP release from AF cells. This graph illustrates the fold change in ATP release from AF cells with respect to uncompressed samples following dynamic compression. 1 Hz and 2 Hz dynamic strain significantly increased ATP release with respect to control samples ($p < 0.05$). Increase seen due to 0.1 Hz compression was not statistically significant. All measurements were normalized to DNA content per sample to account for variation in cell number.

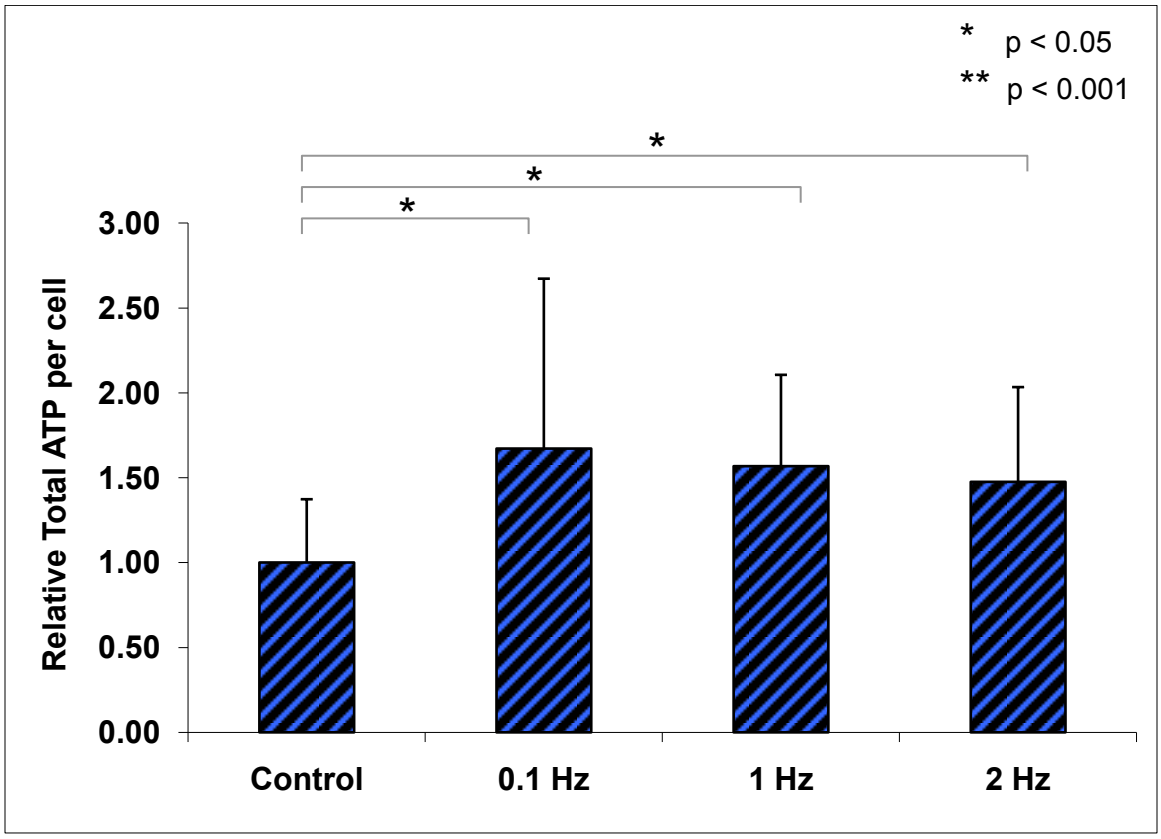

Figure 4- 8: Effects of dynamic loading on total ATP of AF cells. Total ATP in AF cells was significantly increased following dynamic compression at all tested frequencies ($p < 0.05$). However, there were no significant differences observed within the dynamic loading groups. All data were normalized to DNA content per sample to account for variation in cell concentrations.

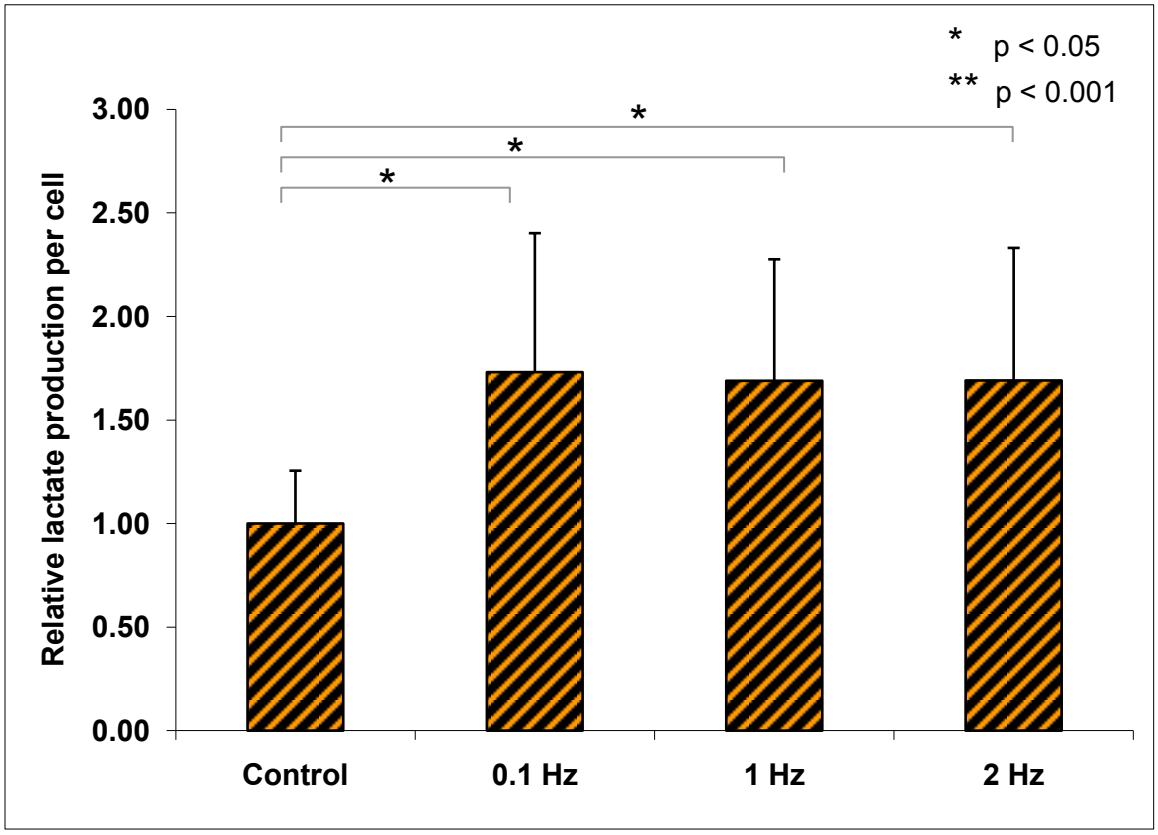

Figure 4- 9: Effects of dynamic loading on lactate production of AF cells. Lactate production of AF cells was significantly increased by dynamic compression at all tested frequencies ($p < 0.05$). However, no significant differences were observed due to the frequency of compression. All data were normalized to DNA content per sample to account for variation in cell number per sample.

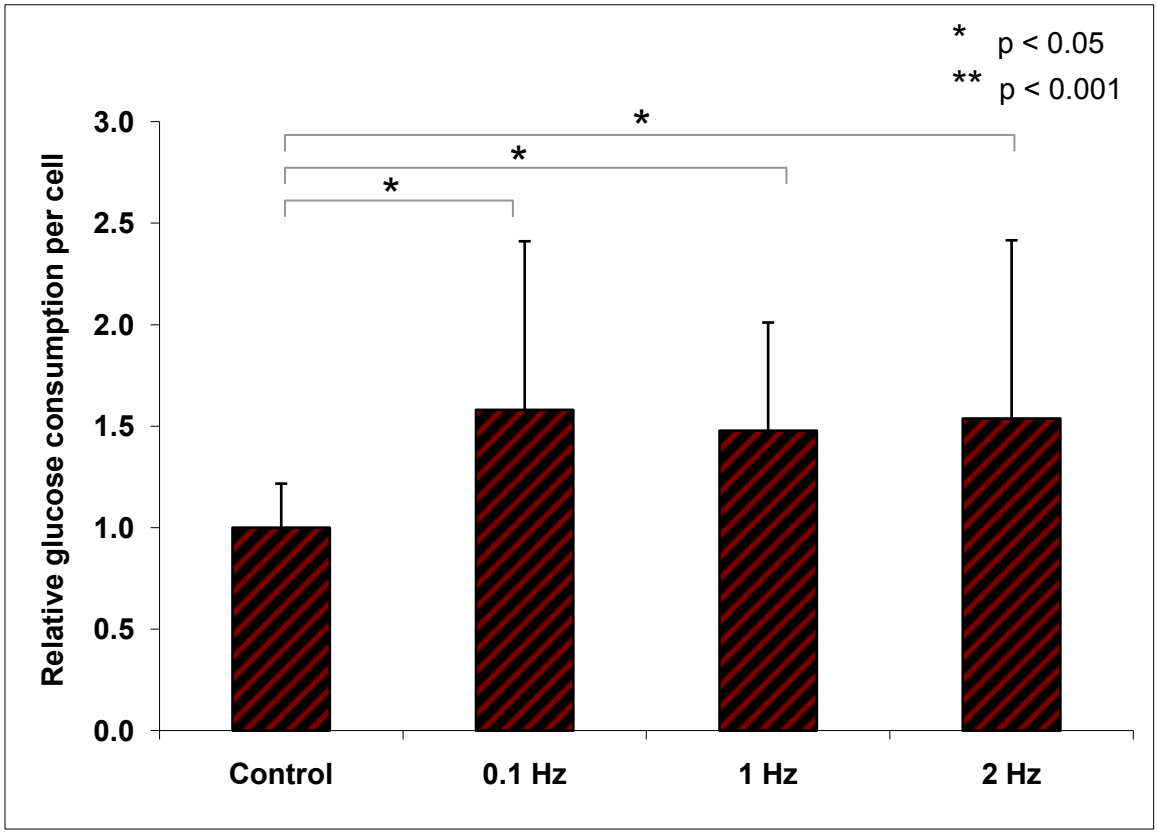

Figure 4- 10: Effects of dynamic loading on glucose consumption of AF cells. Total glucose consumption was calculated based on the change in glucose concentration over the entire loading period and was normalized to DNA content per sample. Glucose consumption was significantly increased in all dynamically compressed groups with respect to uncompressed samples ($p < 0.05$). However, there were no significant differences in glucose consumption between different frequency groups.

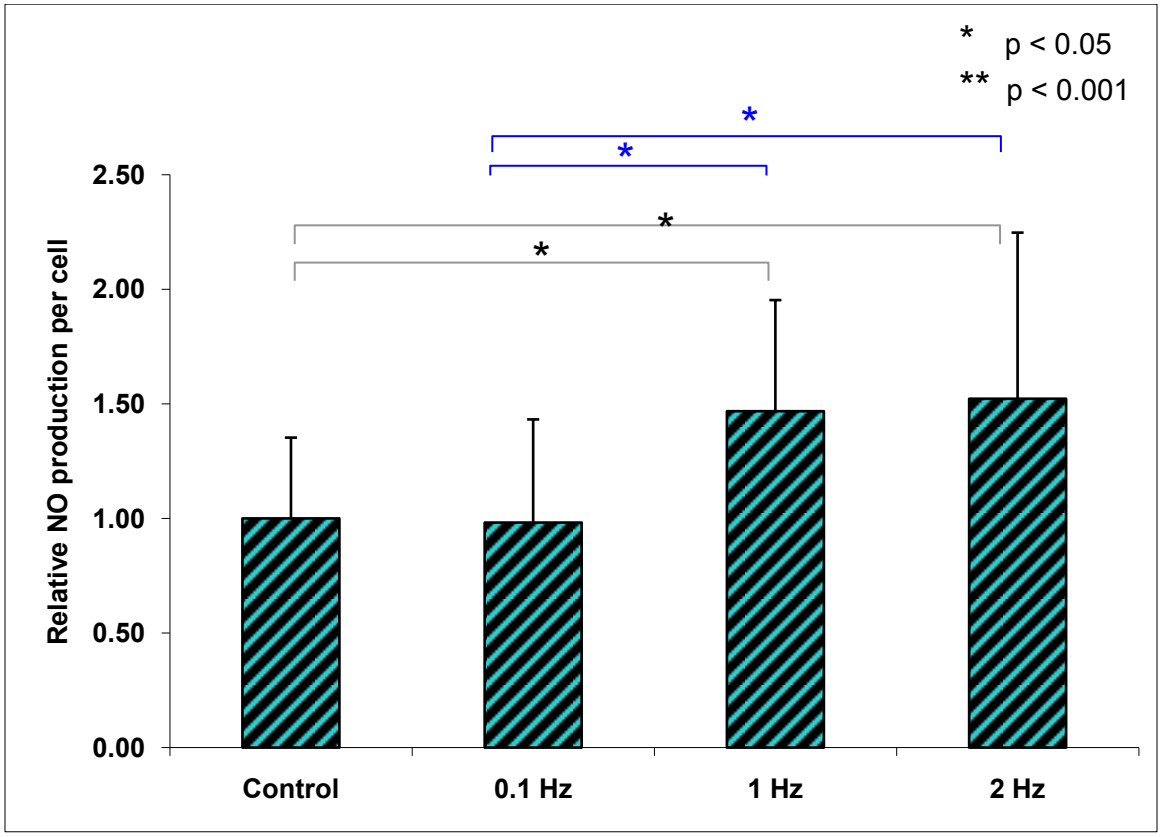

Figure 4- 11: Effects of dynamic compression on NO production of AF cells. NO production of AF cells was significant increased by 1 Hz and 2 Hz dynamic loading groups with respect to control ($p < 0.05$). This increase was also significantly higher compared to 0.1 Hz ($p<0.05$). All data points were normalized to DNA content per sample to account for change in cell number per sample.

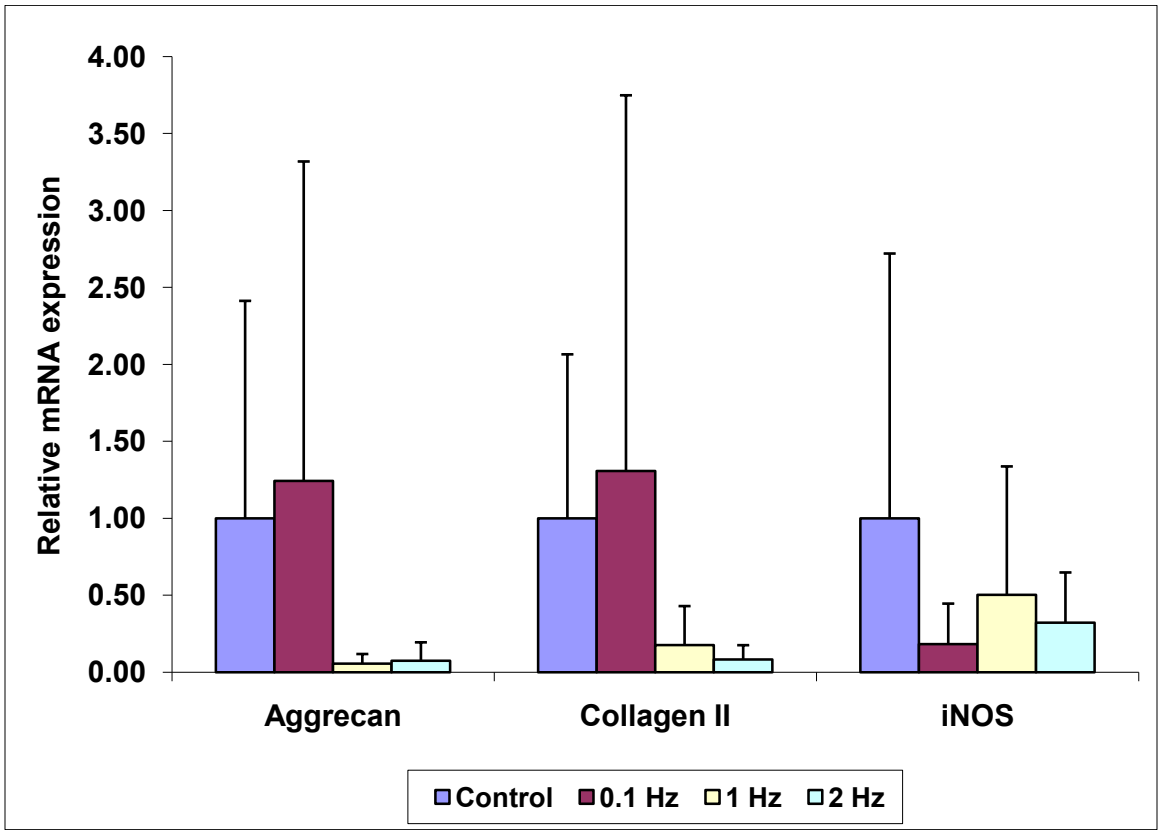

Figure 4- 12: Effects of dynamic loading on extracellular matrix genes of AF cells. All cDNA samples were normalized to 18s internal control and then to respective control samples. Due to significant standard deviation, no significant differences were observed in relative gene expressions.

4.2.1: Effect of static loading on NP cells

ATP release was significantly increased by 30% static strain magnitude but not by 15% strain level with respect to control ($p < 0.001$) [Figure 4- 13]. There were no significant differences observed in total ATP content between compressed and uncompressed samples [Figure 4- 14]. Although an increase in total ATP is seen at 15% static strain level, this increase was not statistically significant. Relative to control, lactate production increased significantly at 15% static compression but not at 30% static compression ($p < 0.05$) [Figure 4- 15]. Significant increases in glucose consumption ($p < 0.05$) [**Figure 4- 16**] and NO production ($p < 0.05$) [**Figure 4- 17**] were observed at both strain levels compared to control.

Statistical analysis of variance between 15% and 30% demonstrated a significant increase in ATP release ($p < 0.001$) [Figure 4- 13] and a significant decreased lactate production ($p < 0.05$) [Figure 4- 15] due to increase in strain level. There were no significant differences in total ATP content, glucose consumption or NO production due to change in strain level.

Static compression of NP cells did not produce a significant variation in mRNA levels of aggrecan, type II collagen and iNOS [Figure 4- 18].

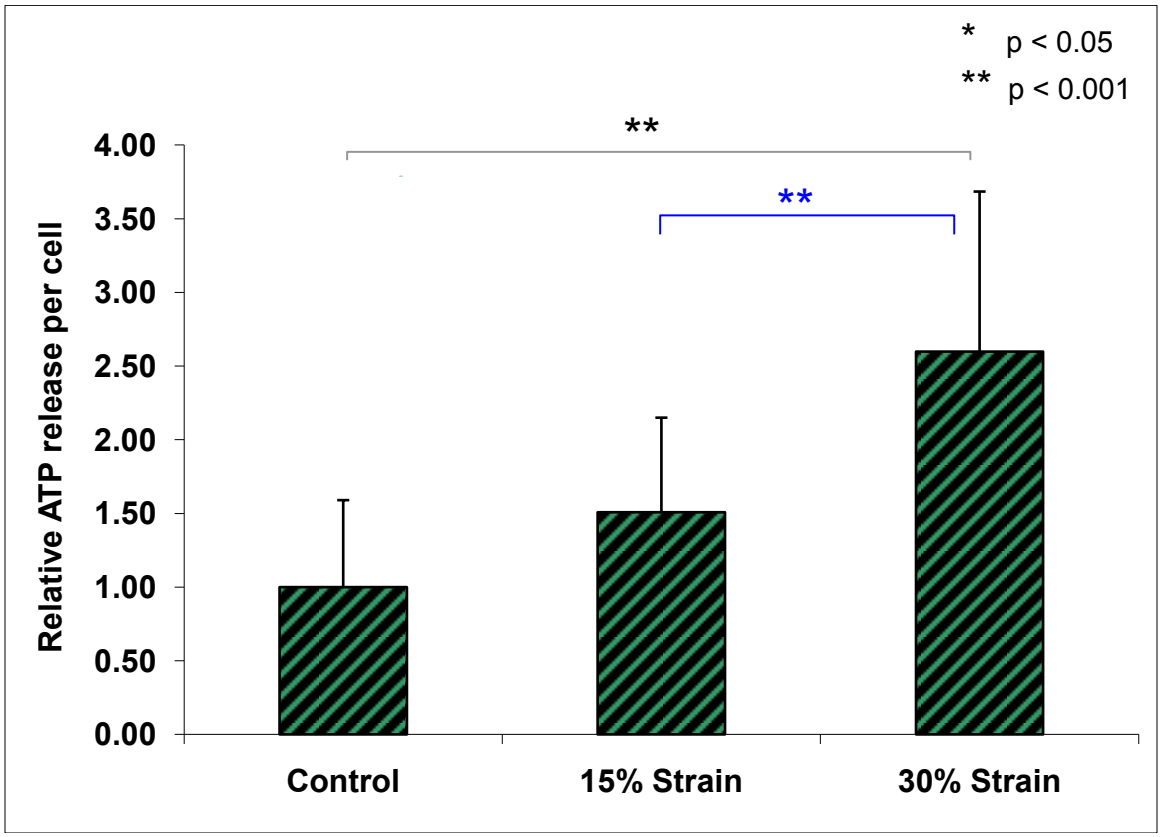

Figure 4- 13: Effects of static loading on ATP release of NP cells. ATP release was significantly promoted by static compression at 30% strain amplitude but not at 15% strain amplitude ($p < 0.001$). Increase in ATP release due at 30% static compression was significantly higher with respect to 15% static compression ($p < 0.001$). All data were normalized to DNA content per sample to account for variation in cell number per sample.

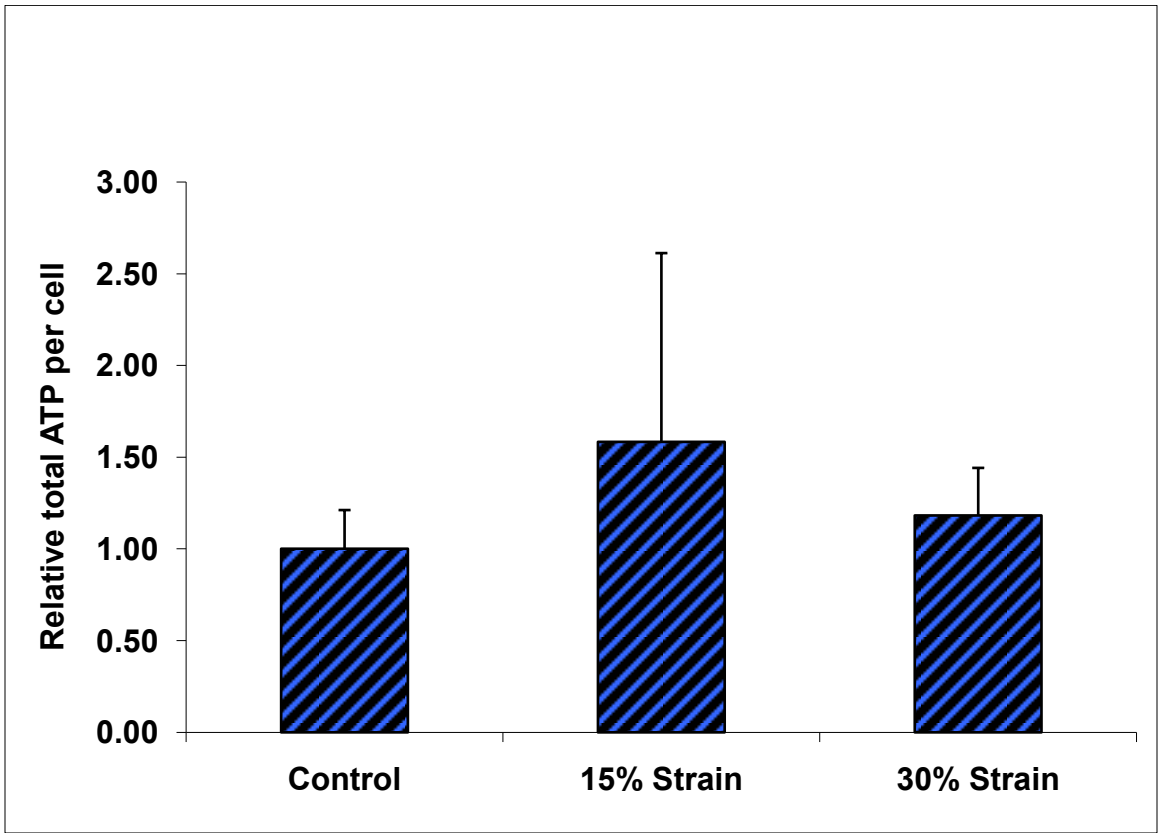

Figure 4- 14: Effects of static loading on total ATP in NP cells. Total ATP content in NP cells were not significantly affected by static compression at either strain level. All data points were normalized to DNA content per sample to account for change in cell number.

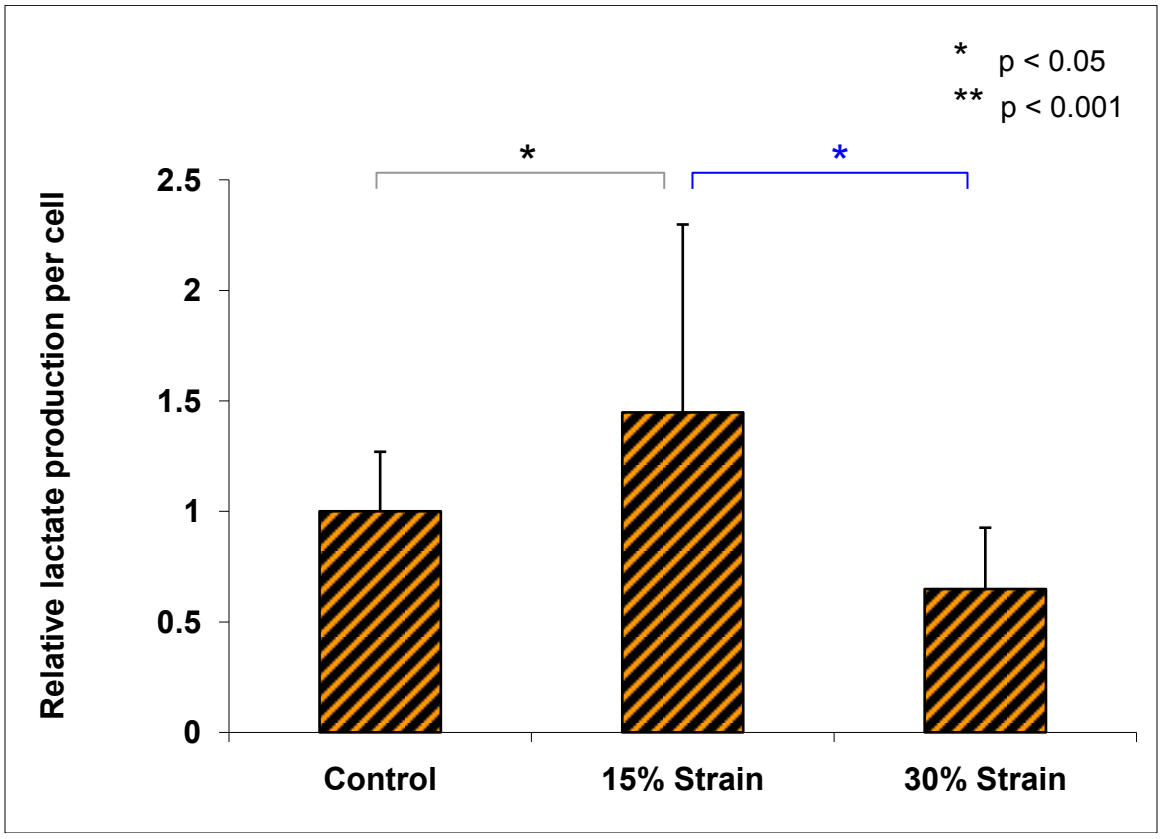

Figure 4- 15: Effects of static loading on lactate production of NP cells. 15% static compression significantly increased lactate production of NP cells with respect to control and 30% static strain magnitude ($p < 0.05$). There were no significant differences between control samples and samples compressed at 30% strain magnitude. All data points were normalized to DNA content per sample to account for variation in cell number per sample.

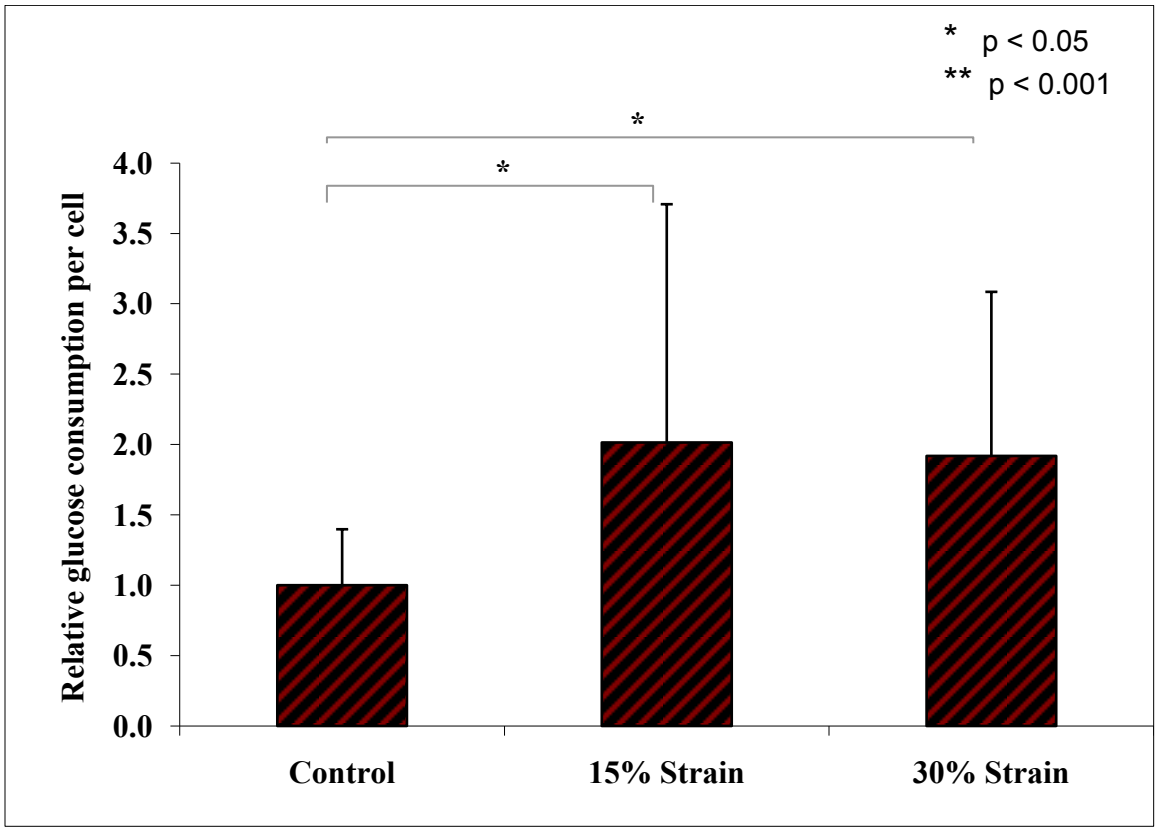

Figure 4- 16: Effects of static compression on glucose consumption of NP cells. Total glucose consumption was calculated based on the change in glucose concentration and was normalized to DNA content per sample. Glucose consumption was significantly increased by both static strain magnitudes with respect to uncompressed samples ($p < 0.05$).

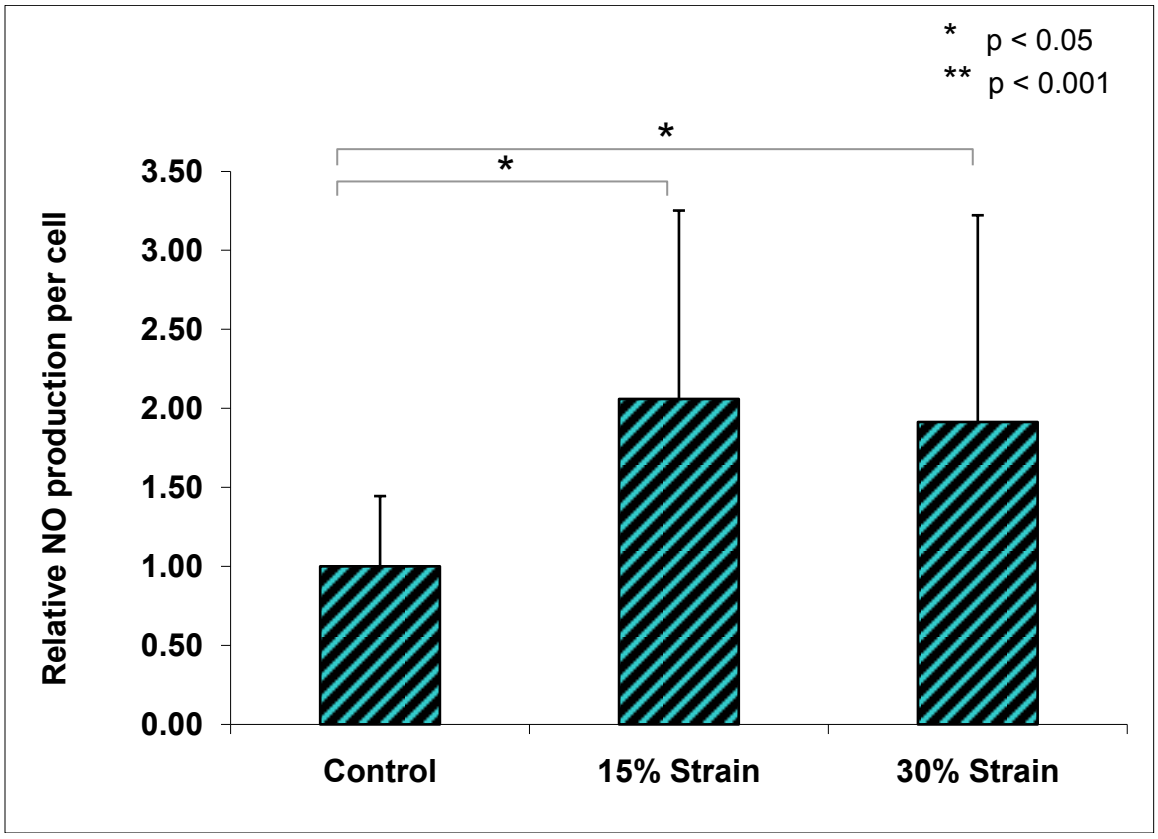

Figure 4- 17: Effects of static loading on NO production of NP cells. NO production was significantly promoted by static compression at both strain magnitudes ($p < 0.05$). There were no significant differences in NO production between samples due to change in strain magnitude.

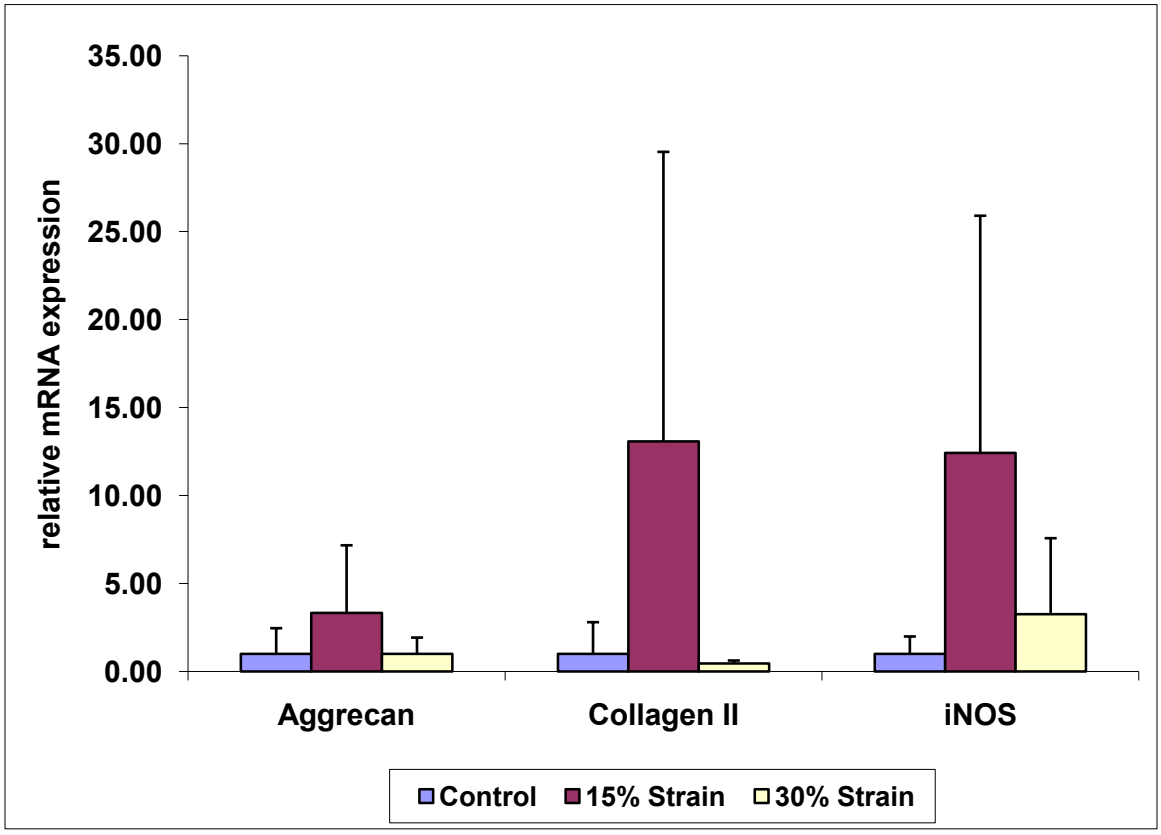

Figure 4- 18: Effects of static compression on extracellular matrix genes in NP cells. All cDNA samples were normalized to 18s internal control and then to respective control samples. Due to significant standard deviation, no significant differences were observed in relative gene expressions.

4.2.2 Effects of dynamic compression on NP cells

Dynamic loading at 1 Hz and 2 Hz significantly increased ATP release relative to control ($p < 0.05$). There were no significant differences in ATP release between 0.1 Hz compressed samples and uncompressed samples [**Figure 4- 19**]. Total ATP in NP cells following 1 Hz dynamic compression was significantly higher relative to uncompressed samples ($p < 0.05$). The increased total ATP detected in other dynamically compressed samples relative to control was not statistically significant [**Figure 4- 20**]. 0.1 Hz dynamic compressed group exhibited significant increase in lactate production relative to control ($p < 0.05$). There were no statistically significant changes in lactate production among uncompressed samples and samples compressed at higher frequencies (1 Hz and 2 Hz) [**Figure 4- 21**]. Glucose consumption was significantly promoted by 1 Hz dynamic compression relative to control ($p < 0.05$). Although an increase in glucose consumption relative to control is detected in 0.1 Hz and 2 Hz compressed samples, these changes were not statistically significant [**Figure 4- 22**]. NO production of NP cells was significantly promoted by all tested dynamic frequencies ($p<0.001$) [**Figure 4- 23**].

Dynamic loading frequency dependence was observed in ATP release and NO production of NP cells. Increase in ATP release at 1 Hz and 2 Hz was statistically significant relative to 0.1 Hz dynamic compression ($p < 0.05$) [**Figure 4- 19**]. Increase in NO production at 1 Hz was significantly higher compared to 0.1 Hz and 2 Hz dynamic compression ($p < 0.001$) [**Figure 4- 23**].

Dynamic compression of NP cells did not produce a significant variation in mRNA levels of aggrecan, type II collagen and iNOS [Figure 4- 24].

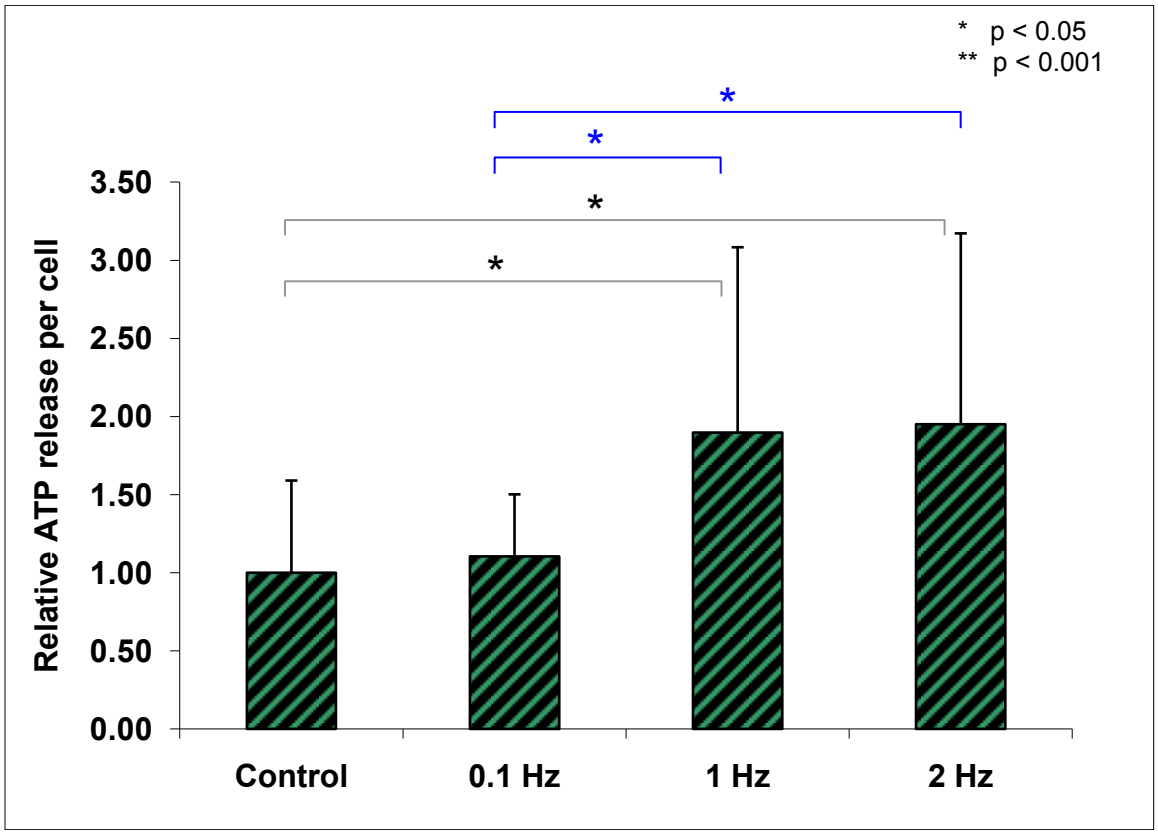

Figure 4- 19: Effects of dynamic loading on ATP release from NP cells. ATP release from NP cells was significantly promoted by dynamic compression at 1 Hz and 2 Hz relative to control ($p < 0.05$). This increase was also significant relative to ATP release from NP cells compressed at 0.1 Hz ($p < 0.05$). There were no significant differences between uncompressed samples and samples dynamically compressed at 0.1 Hz. All data points were normalized to DNA content per sample to account for variation in cell number per disk.

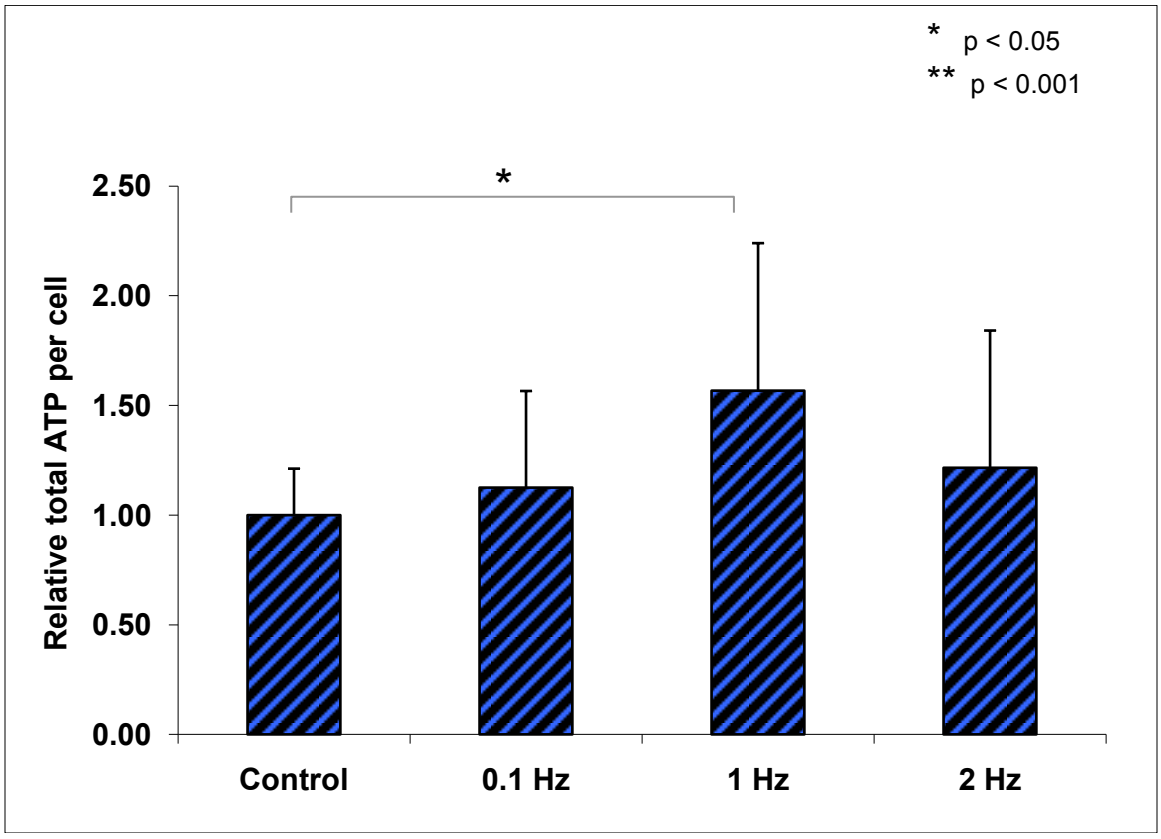

Figure 4- 20: Effects of dynamic compression on total ATP of NP cells. Significant increase in total ATP relative to control was observed in samples compressed at 1 Hz ($p < 0.05$). Although the data suggests an increase in total ATP in other dynamic loading groups, these were not statistically significant. All data were normalized to DNA content per sample to account for variation in cell number per sample. The bar graphs indicate the fold change relative to control.

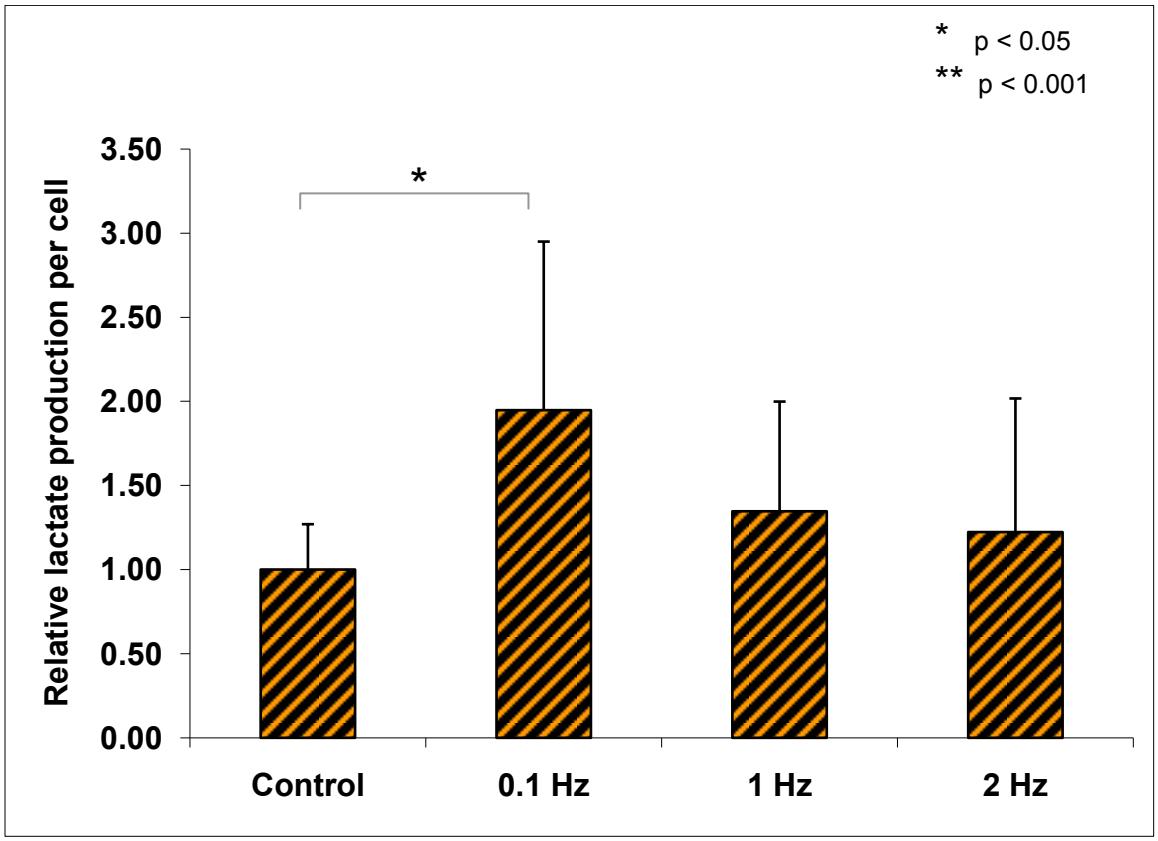

Figure 4- 21: Effects of dynamic loading on lactate production of NP cells. Lactate production of NP cells was significantly increased by 0.1 Hz relative to control ($p < 0.05$). The increases relative to control seen in other dynamically compressed groups were not statistically significant. There was no frequency dependence in lactate production of NP cells. All data points were normalized to DNA content per sample to account for variation in cell number. The bar graphs illustrate the fold change relative to control.

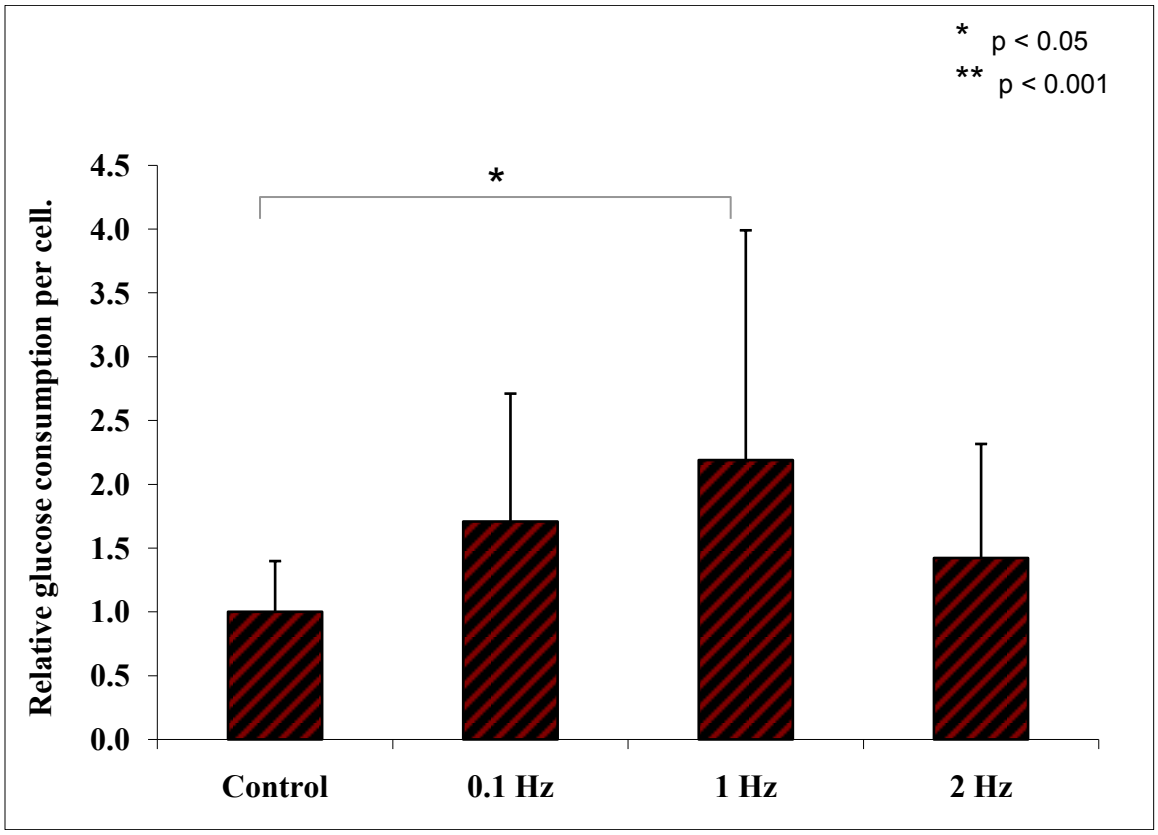

Figure 4- 22: Effects of dynamic loading on glucose consumption of NP cells. Total glucose consumption was calculated based on the change in glucose concentration over the entire length of the experiment and was normalized to DNA content per sample. Glucose consumption was significantly increased by 1 Hz dynamic compression relative to control ($p < 0.05$). The increases relative to control seen in other dynamically compressed groups were not statistically significant.

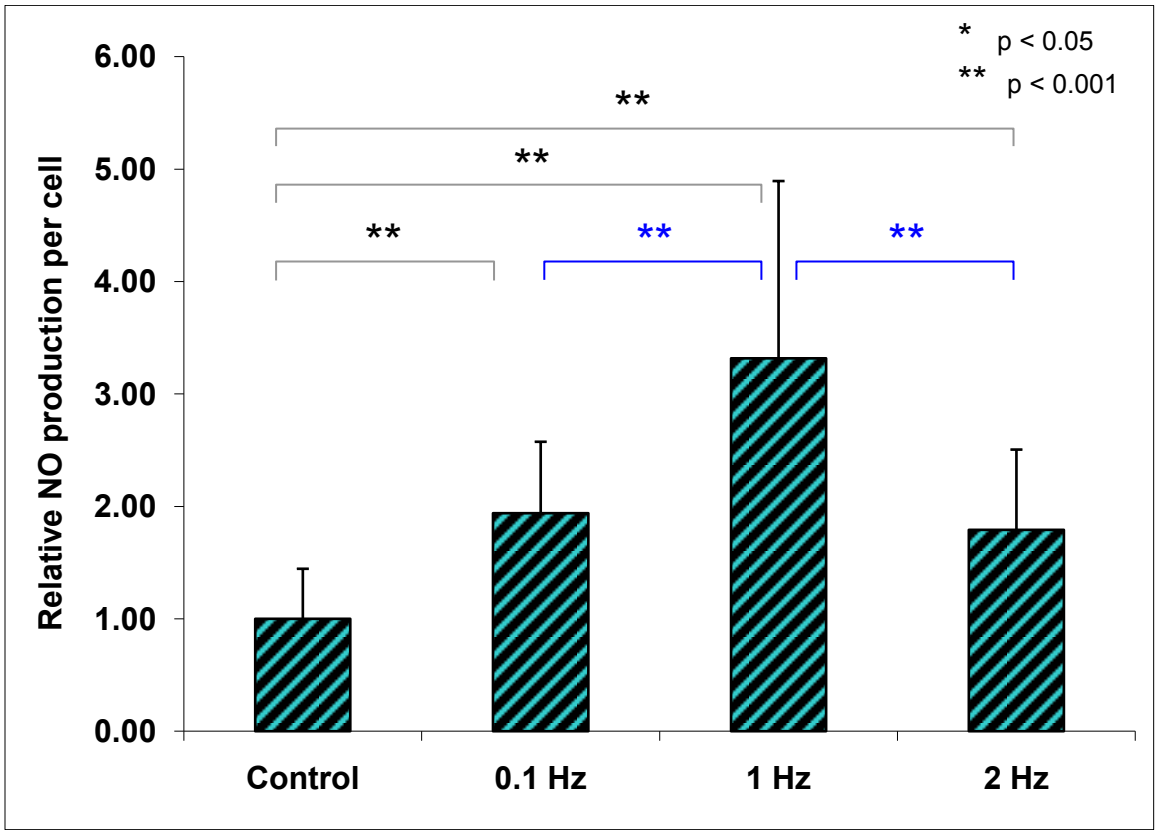

Figure 4- 23: Effects of dynamic loading on NO production of NP cells. All tested dynamic frequencies up regulated NO production of NP cells relative to control ($p<0.001$). NO production due to 1 Hz dynamic loading was significantly higher respect to other dynamic loading groups ($p<0.001$). All data points were normalized to DNA content per sample to account for variation in cell number. The bar graphs indicate the fold increase relative to control group.

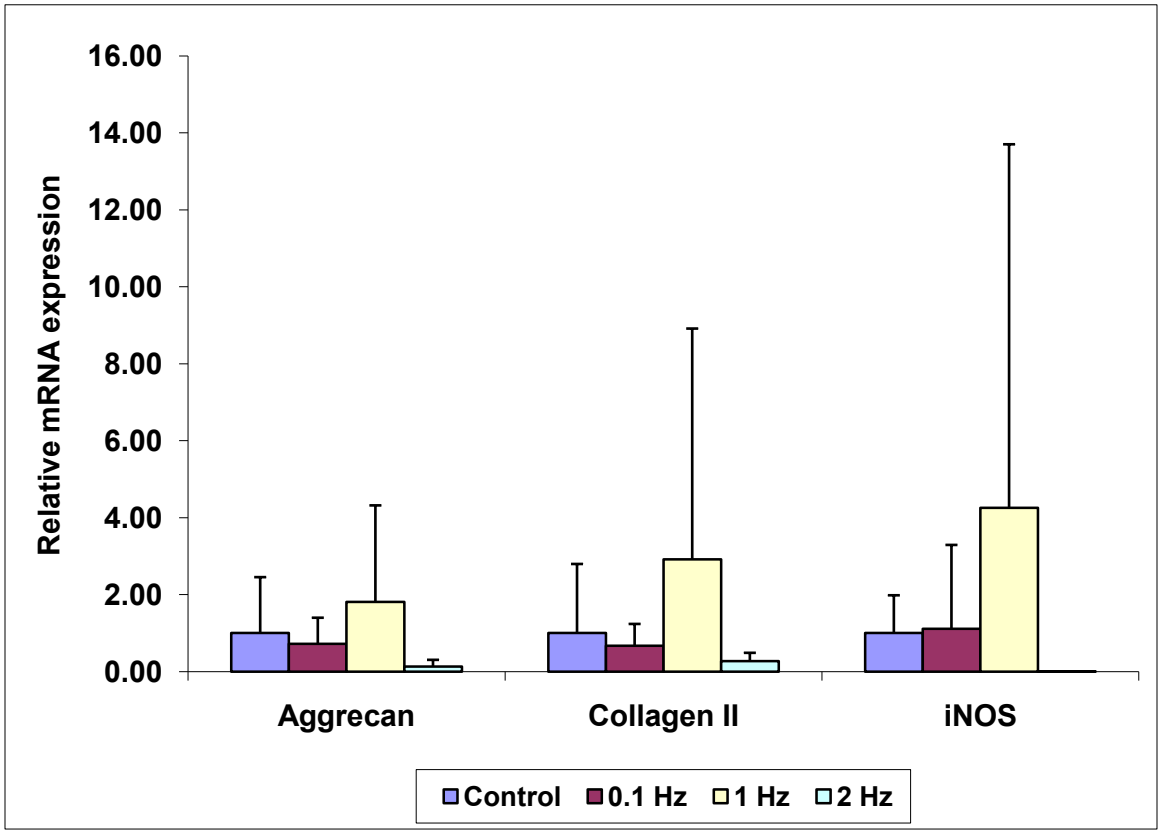

Figure 4- 24: Effects of dynamic compression on extracellular matrix genes in NP cells. All cDNA samples were normalized to 18s internal control and then to respective control samples. Due to significant standard deviation, no significant differences were observed in relative gene expressions.

4.3.1: Comparison between AF and NP cells

At control culture conditions, NP cells had a significantly higher total ATP content ($p < 0.001$) and significantly lower glucose consumption ($p < 0.001$), lactate production ($p < 0.001$) and NO production ($p < 0.001$) relative to AF cells. However, there were no differences in ATP release between AF and NP cells at control conditions [**Figure 4- 25**].

At 15% static compression, NP cell ATP content ($p<0.001$) and ATP release by NP cells ($p < 0.001$) were significantly higher than those of AF cells. Lactate production ($p < 0.001$), glucose consumption ($p < 0.001$) and NO production ($p < 0.001$) remained significantly lower in NP cells relative to AF cells [**Figure 4- 26**].

Following 30% static compression, NP cell ATP content ($p < 0.001$) and ATP released by NP cells ($p < 0.05$) were higher compared to AF cells. Lactate production ($p < 0.001$), NO production ($p < 0.05$) and glucose consumption ($p < 0.001$) remained significantly lower in NP cells at this static strain level [**Figure 4- 27**].

Total ATP content in NP cells were significantly higher compared to AF cells in all dynamic compression groups ($p < 0.001$ for all frequencies). Additionally, glucose consumption ($p < 0.001$ all groups), lactate production (0.1 Hz, 1 Hz: $p < 0.05$; 2 Hz: $p < 0.001$) and NO production ($p < 0.001$ all groups) remained significantly lower in NP cells compared to AF cells under respective dynamic loading group. ATP release by NP cells was significantly lower compared to AF cells at 0.1 Hz ($p < 0.05$). However, this relation was reversed at 2 Hz where ATP release from NP cells was significantly higher compared to AF cells ($p < 0.05$). There were no statistically significant differences in

ATP release at 1 Hz between AF and NP cells [**Figure 4- 28**; **Figure 4- 29**; **Figure 4-30**].

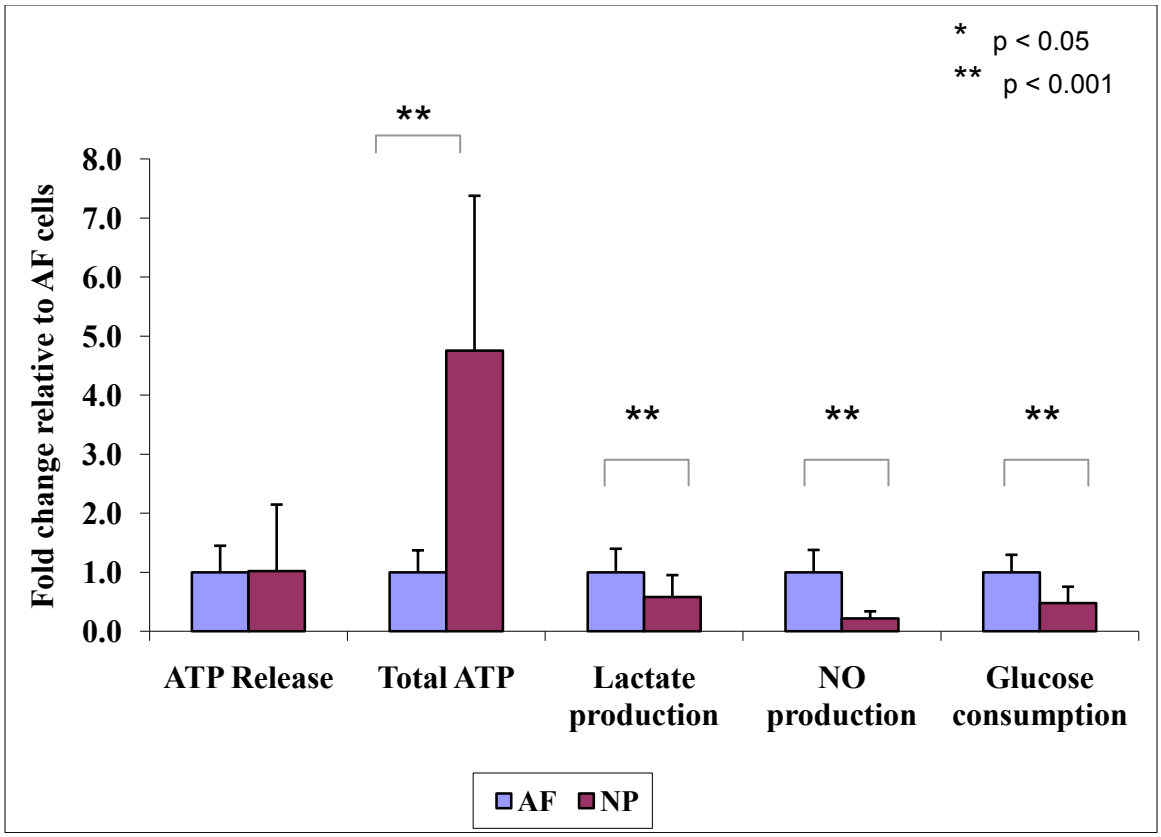

Figure 4- 25: Comparison of AF and NP cells at control culture conditions. There were no significant differences in ATP release between AF cells and NP cells under control culture conditions. While the total ATP was significantly higher in NP cells, lactate production, NO production and glucose consumption remained significantly lower in AF cells relative to NP cells ($p < 0.001$ for all measurements). All data points were first normalized to DNA content per sample to account for variation in cell number. The bar graphs indicate the fold change of each assay relative to AF cells.

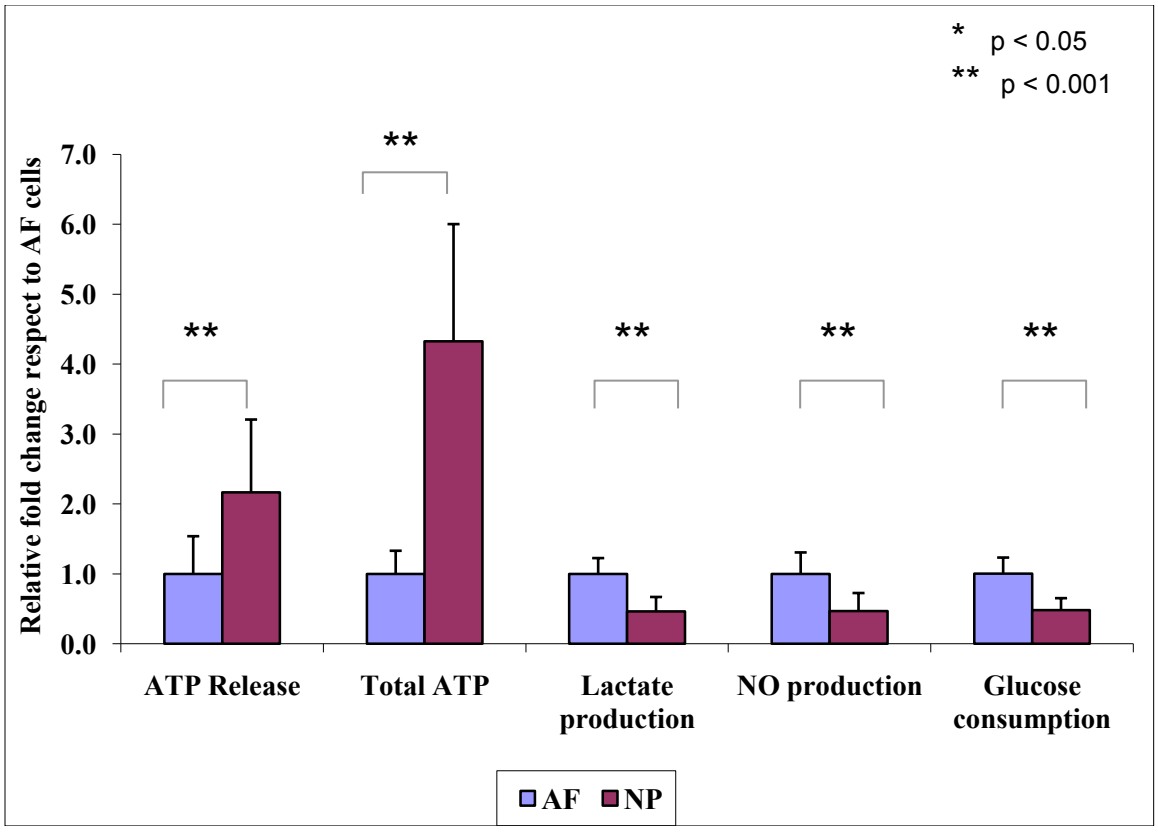

Figure 4- 26: Comparison of AF and NP cells following 15% static compression. ATP release and total ATP in NP cells were significantly higher compared to AF cells following 15% static compression ($p < 0.001$). Lactate production, NO production and glucose consumption remained significantly lower in NP cells compared to AF cells ($p < 0.001$ all measurements). All data points were first normalized to DNA content per sample to account for variation in cell number. The bar graphs indicate the ratio between AF and NP cells for respective assays.

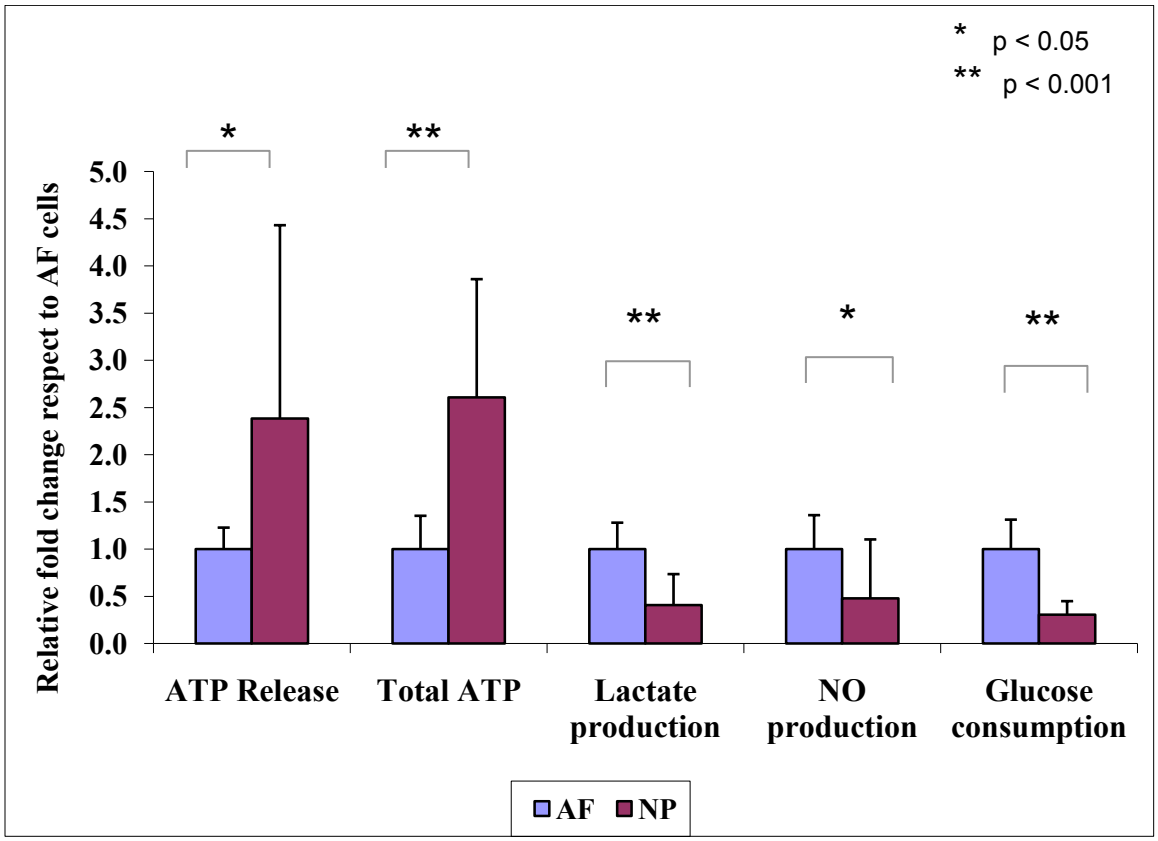

Figure 4- 27: Comparison of AF and NP cells following 30% static compression. ATP release and total ATP was significantly higher in NP cells relative to those of AF cells ($p < 0.001$). Lactate production, NO production and glucose consumption remained significantly lower in NP cells compared to AF cells ($p < 0.001$ all measurements). All data points were first normalized to DNA content per sample to account for variation in cell number. The bar graphs indicate the ratio between AF and NP cells for respective assays.

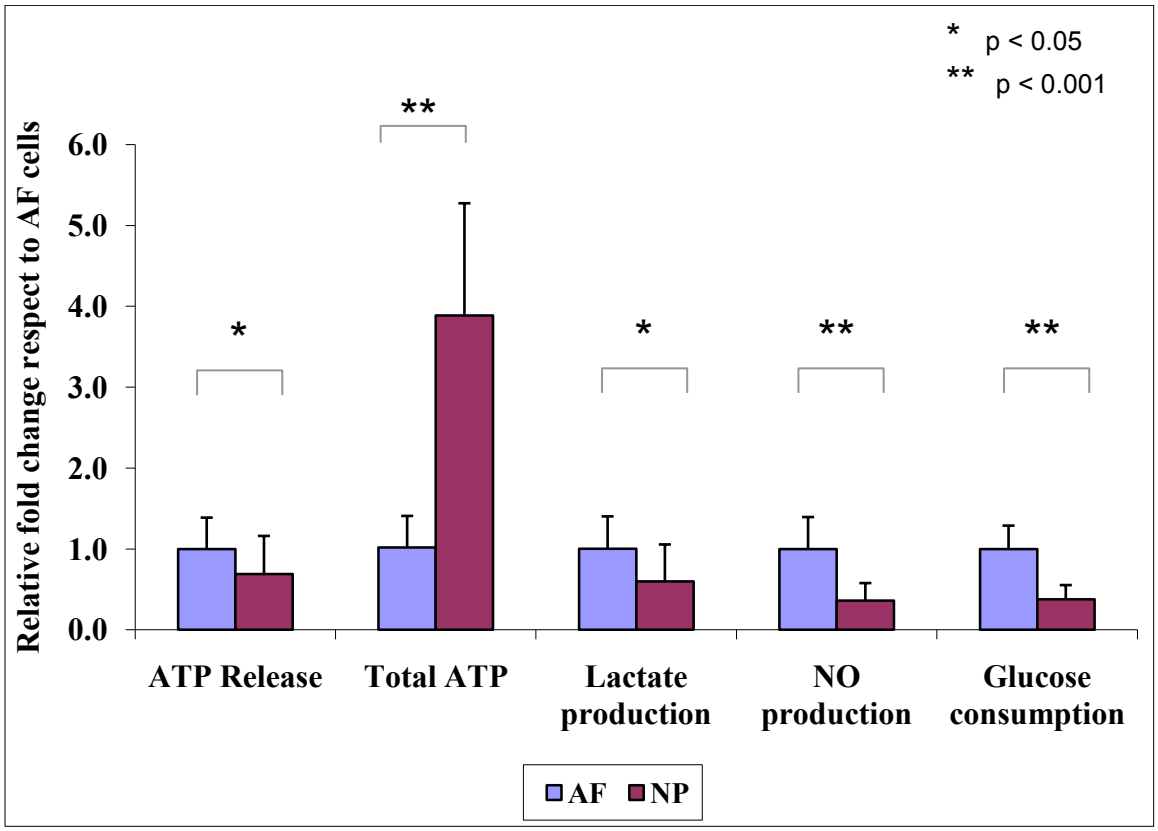

Figure 4- 28: Comparison of AF and NP cells following 0.1 Hz dynamic compression. Total ATP of NP cells was significantly higher relative to AF cells ($p < 0.001$). ATP release ($p < 0.05$), lactate production ($p < 0.05$), NO production ($p < 0.001$) and glucose consumption ($p < 0.001$) remained significantly lower in NP cells compared to AF cells. All data points were first normalized to DNA content per sample to account for variation in cell number. The bar graphs indicate the ratio between AF and NP cells for respective assays.

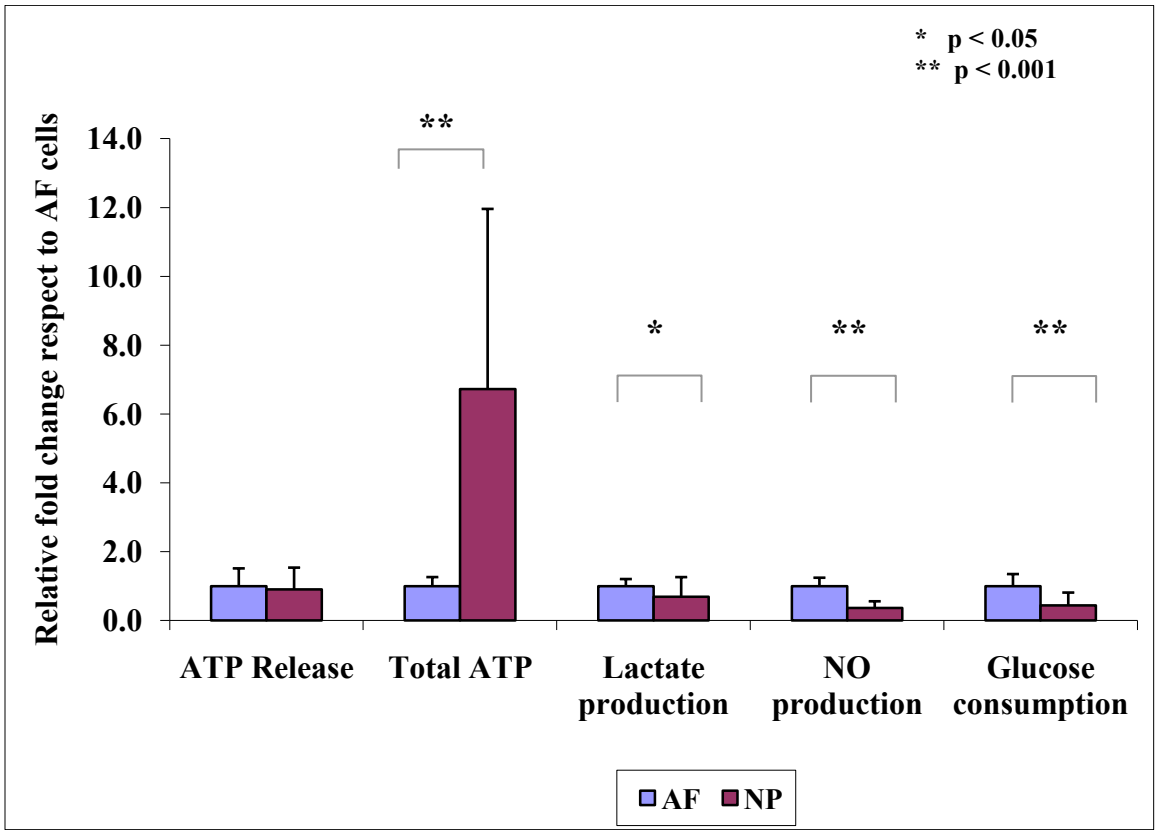

Figure 4- 29: Comparison of AF and NP cells following dynamic compression at 1 Hz. Total ATP of NP cells was significantly higher relative to AF cells ($p < 0.001$). There were no significant differences in ATP release between AF and NP cells at this compression. Lactate production ($p < 0.05$), NO production ($p < 0.001$) and glucose consumption ($p < 0.001$) remained significantly lower in NP cells compared to AF cells. All data points were first normalized to DNA content per sample to account for variation in cell number. The bar graphs indicate the ratio between AF and NP cells for respective assays.

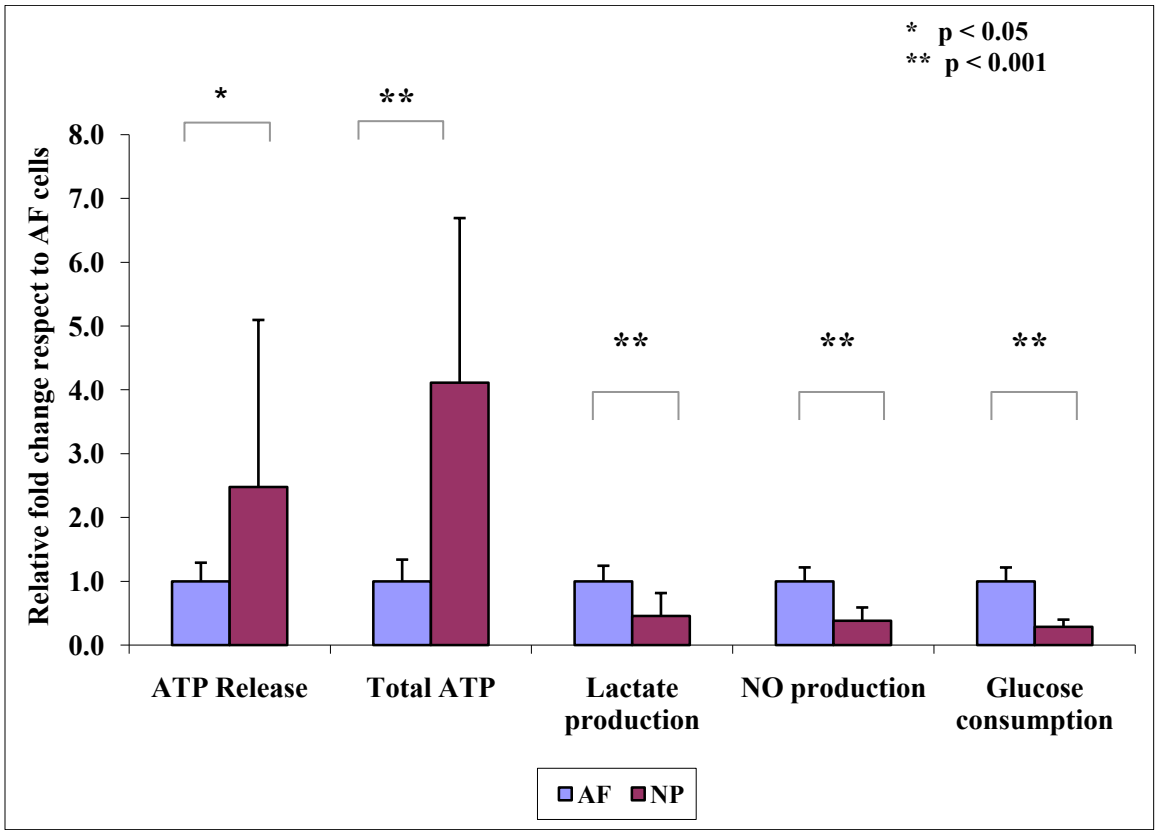

Figure 4- 30: Comparison of AF and NP cells following dynamic compression at 2 Hz. ATP release ($p < 0.05$) and total ATP ($p < 0.001$) of NP cells was significantly higher relative to AF cells. Lactate production, NO production and glucose consumption remained significantly lower in NP cells compared to AF cells ($p < 0.001$ all measurements). All data points were first normalized to DNA content per sample to account for variation in cell number. The bar graphs indicate the ratio between AF and NP cells for respective assays.

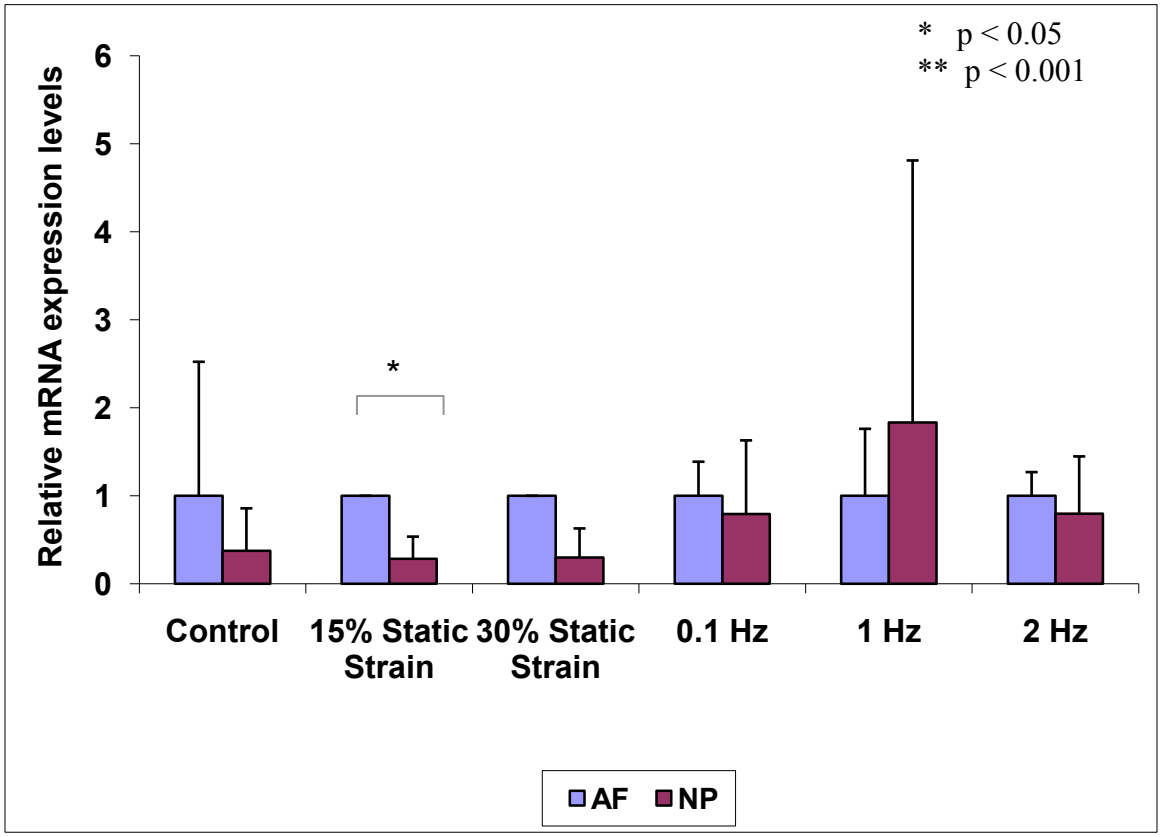

Figure 4- 31: Comparison of aggrecan expression in AF and NP cells at different culture conditions. NP cells displayed a significantly lower level of aggrecan at 15% static compression ($p < 0.05$). There were no significant differences in aggrecan expression levels at other testing conditions. All samples were normalized to 18s to account for variation in cDNA per sample and then normalized to respective AF sample.

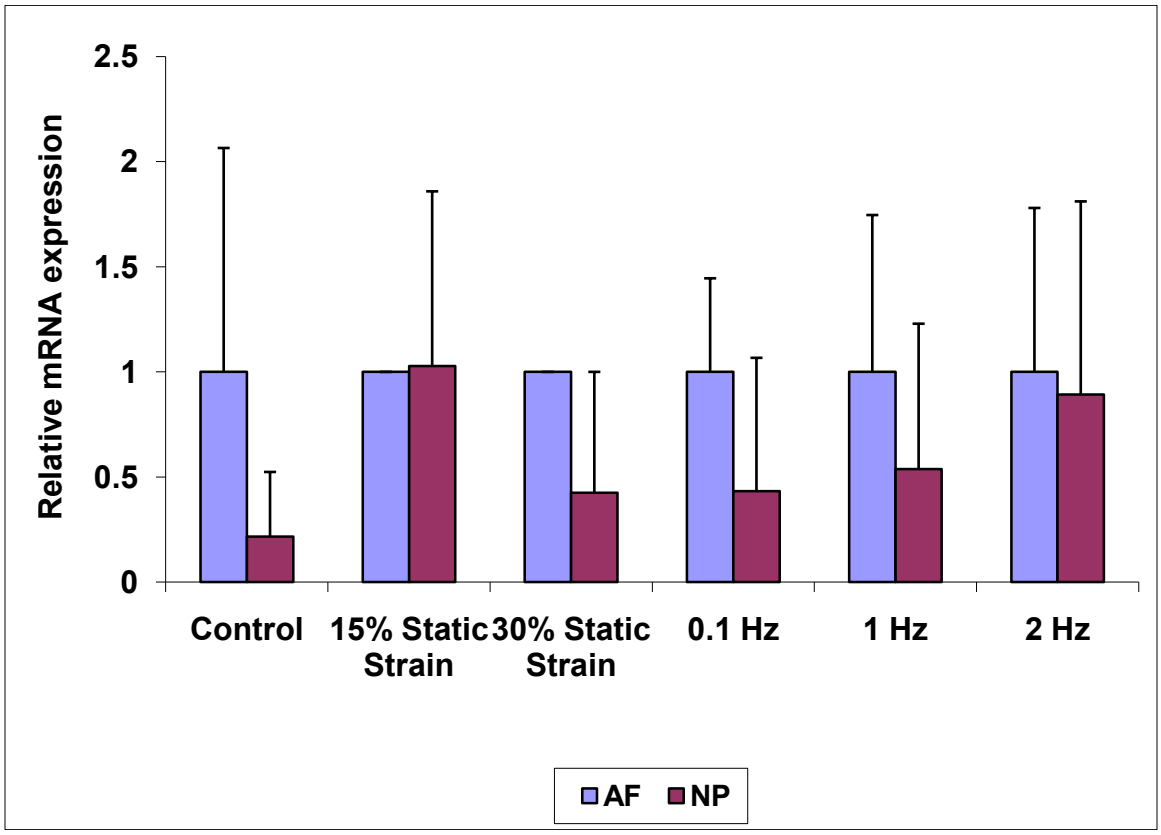

Figure 4- 32: Comparison of type II collagen expression in AF and NP cells at different culture conditions. There were no significant differences in type II collagen expression at all tested conditions. All samples were normalized to 18s to account for variation in cDNA per sample and then normalized to respective AF sample.

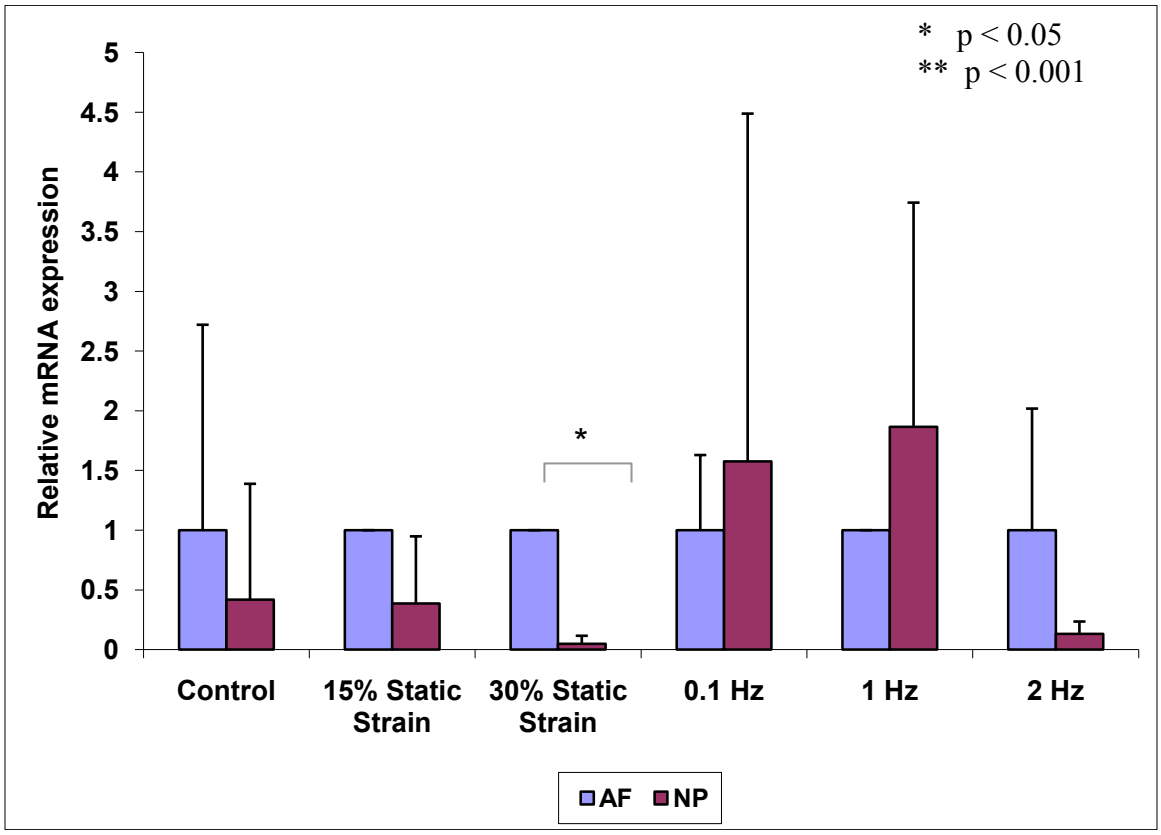

Figure 4- 33: Comparsion of iNOS expression in AF and NP cells at different culture conditions. NP cells exhibited a significant decrease in iNOS expression following 30% static compression ($p < 0.05$). There were no significant differences in iNOS expression levels in other tested conditions. All samples were normalized to 18s to account for variation in cDNA per sample and then normalized to respective AF sample.

Chapter 5: DISCUSSION

IVD is an important structural and functional unit of the spine. Degeneration of the IVD is closely linked to low back pain, a major socio-economic burden in the USA [1]. This association has stimulated researches to identify degenerative processes of the IVD. Among multiple possible causes, inefficient nutrient supply to IVD takes the lead [18]. Given the constant exposure to mechanical loading of the spine, many studies are conducted to understand how mechanical loading affect IVD tissue regulation at a cellular and tissue level [5,26,28,32,36,37,39,45,57,80,86,91]. While a correlation between mechanical loading and IVD biosynthesis is seen, the signaling pathway(s) to this effect is still unknown. Additionally, a study conducted by Lee et al. on cartilage demonstrated that cellular biosynthesis can be affected by mechanical loading due to change in ATP turnover [52]. We suspect a similar effect on IVD energy metabolism due to mechanical loading. A previous study conducted in our lab evaluated the effects of dynamic loading at 2 Hz on energy metabolism of IVD cells. To our knowledge, this is the first study to evaluate the effects of static compressive mechanical loading and multiple compressive dynamic loading frequencies on energy metabolism of IVD cells.

5.1: Justification of experiment model

Previously it was shown that phenotype of IVD cells changes in sub-culturing [12]. To eliminate the effects of these phenotypic changes, fresh porcine cells were used for this experiment. Further, cells were suspended in 2% agarose gel to mimic its 3-dimentional microenvironment and retain its phenotype throughout the experiment.

Based on theoretical studies, 2% agarose was shown to exhibit isotropic properties and have minimal effects on transport of small solutes [23,24]. Thus variations in energy metabolism due to changes in nutrient supply to cells were eliminated in this study. Also, we believe at the given dimensions of the agarose disk, it is able to produce uniform force distribution to all cells within construct [63].

During daily activities, human spine is subjected a wide range of motions. A study showed that at rest the human IVD is subjected to approximately 0.19 MPa pressure while a disc pressure above 3 MPa may cause vertebral fracture [76]. Equivalently, physiological frequency of the human spine has a wide range with resonance occurring around 4 – 6 Hz at the lumbar spine region [49]. Even at rest, IVD tissue is subjected to pressure due to gravity and counteracting forces exerted by various muscles and ligaments to maintain posture. Due to this wide range in mechanical loading parameters (strain level, duration, frequency), we conducted two strain levels (15% and 30%) to understand the effects of increased strain on IVD cells in static compression. Agarose gels were unable to maintain structural integrity at 30% strain under dynamic loading, and as a result only 15% dynamic strain was evaluated. Three frequency levels within physiological range were tested: 0.1 Hz, 1 Hz and 2 Hz. 4 hr duration was chosen based on practicality in carrying out all loading experiments and was thought to be reasonable based on a previous study conducted in our lab in which changes in mesenchymal stem cell biosynthesis was altered following 4 hr compression [33]. However, the future studies will evaluate the effects of duration on energy metabolism of IVD cells under compression.

Various studies have shown that cells release ATP in response to mechanical stimulation. Therefore we measured ATP concentrated in sample medium to scope the change in ATP release under different loading regimes. Total ATP, which combined intracellular ATP and ATP released to medium, was used to evaluate ATP production. Lactate production was measured as a reference for ATP production via lactic acid pathway, a major metabolic pathway for IVD cell ATP production.

NO, a potent inhibitor of oxidative phosphorylation was measured to evaluate potential changes to mitochondrial respiration in IVD cells under mechanical compression. Studies have also shown that NO production is up regulated by shear stress induced by fluid flow and mechanical stretch in various cell types [29,41,66,72]. However, a study conducted by Lee et al. demonstrated that dynamic compression of bovine chondrocytes suppressed NO production [51]. Although NO concentration was measured in both media and cell-agarose construct in a preliminary experiment, NO concentration in gel was negligible (data not shown), and as such only medium concentration was evaluated for successive experiments.

A live-dead staining was conducted in a preliminary experiment to ensure cells remained viable at the end of each loading experiment. Cell-agarose constructs showed greater than 98% viability confirming tested conditions were not fatal to cells (data not shown). All measurements were normalized to sample DNA content to account for cell number variation per sample.

5.2: Experimental findings

5.2.1: Effects of static compression on energy metabolism of IVD cells

In the current study, increased lactate production of AF cells at 15% static compression indicates that, at this strain level, there is a significant increase in ATP production via lactic acid pathway. In our study, although not statistically significant, glucose consumption does exhibit an increase due to static compression. It is likely that this statistical insignificance is due to low sample number failing to produce a statistical significance.

At higher static strain level (30%), increased glucose consumption was not followed by an increased lactate production in AF cells. Lack of differences seen in NO production implies that ATP production via electron transport chain was not affected relative to control at 30% static compression. Increase in glucose consumption and total ATP collectively advocate that ATP synthesis is promoted due to compression; however the path to this effect cannot be easily accounted for. Few theories can be speculated to explain this observation. For example, it is possible that at 30% compression, more pyruvate acid following glycolysis enters mitochondria and contributes to more ATP production. It is important to note that pyruvate acid entering mitochondria can produce 2 more ATP molecules in Krebs cycle by substrate-level phosphorylation (production of ATP by direct transfer of a phosphoryl (PO_3) group from an intermediate metabolite to adenosine di-phosphate - ADP). This pathway would result in increased ATP production without increasing lactate production. Also in addition to ATP synthesis, glucose can be consumed for different cellular processes such as glycosaminoglycan (GAG) synthesis, which would not produce lactate as a byproduct further contributing to the discrepancy in

glucose consumption and lactate production correlation. The explanations presented here however remain strictly hypothetical, and needs to be investigated in future experiments.

Significant increase of lactate production in NP cells indicated that ATP production via lactic acid pathway is up-regulated at 15% static compression. Increase in NO production seen due to 15% static compression might result in inhibition of mitochondrial respiration (i.e., reduction in mitochondrial ATP production). As such, increased glucose consumption and lactate production may be a mechanism to compensate decreased ATP production in mitochondria, and to maintain cellular activities and maintain viability. At 30% static strain level, similar elevation of NO production and glucose consumption was observed. However lactate production was not affected at this strain level. Similar to AF cells subjected to 30% static compression, this increase in glucose consumption and lack of subsequent increase in lactate production can be explained by the possibility of pyruvate acid entering mitochondria following glycolysis. Taken as a whole, data suggests that under static compression (at tested culture conditions), NP ATP synthesis via electron transport is inhibited and is shifted to ATP production via substrate-level phosphorylation. This would result in a decreased ATP yield per glucose molecule compared to control. As such, increased glucose consumption does not guarantee increased ATP production relative to control (which will maintain its normal ATP production via oxidative phosphorylation). This explanation is supported by the lack of differences observed in total ATP content between control and compressed groups.

Previous studies have stated that AF cell response to mechanical loading was primarily strain magnitude dependent while NP cells were responsive to both strain

magnitude and frequency of loading [45,58]. Consistently, in our study, glucose consumption and lactate production of AF cells and lactate production and ATP release of NP cells exhibited strain dependency.

Multiple studies have reported that cellular biosynthesis is optimum at physiological strain levels and tends to decrease outside this range [26,69]. A study conducted by Wang et al showed that cellular biosynthesis decreased with static compression but increased with dynamic compression [88]. Though not directly comparable due to differences in experimental protocols, our data illustrates that ATP production is affected by mechanical loading. Among other factors, it is also possible that changes in cellular biosynthesis under compression are governed by energy supply to the cells.

5.2.2: Effects of dynamic compression on energy metabolism of IVD cells

Lactate production, glucose consumption and total ATP content of AF cells were increased relative to control by all tested dynamic frequencies. This collectively indicates that dynamic compression promotes ATP production of AF cells via lactic acid pathway.

Based on the findings in this study, it is apparent that energy metabolism of NP cells can be complicated compared to that of AF cells. All dynamic loading frequencies exhibit an increase in NO production suggesting a possible inhibition in ATP synthesis via oxidative phosphorylation relative to control. Increase in NO production at 1 Hz was significantly higher with respect to 0.1 Hz and 2 Hz indicating a possible elevated inhibition in ATP production at this frequency level relative to other dynamic loading

groups. Lack of difference in lactate production at 1 Hz with respect to control suggests that the increased glucose consumption does not follow anaerobic respiration, and as suggested before might promote ATP production in mitochondria. Despite a possible inhibition in ATP synthesis by NO, net ATP production of NP cells was up regulated by dynamic loading at 1 Hz.

0.1 Hz dynamic loading exhibited an increased lactate production which suggests that at this frequency, ATP production via lactic acid pathway was promoted in NP cells. Significant increase in NO production relative to control further suggests a possible inhibition of ATP production in mitochondria. As mentioned previously, ATP yield per glucose molecule is much lower via lactic acid pathway than that via mitochondria. Thus, this decrease in ATP yield could explain the lack of difference in total ATP content relative to control. Although glucose consumption was increased at this frequency, this increase was not statistically significant. As such, we are unable to statistically account for glucose molecules contributing to the production of lactate. It is possible however, that lack of significance is directly linked to low sample number.

2 Hz dynamic loading did not produce statistically significant differences in glucose consumption, lactate production or total ATP in NP cells relative to control. However, NO production and ATP release were significantly up-regulated at this dynamic frequency.

Overall, this study clearly demonstrates that dynamic loading affects energy metabolism of IVD cells. While ATP production of AF cells was promoted by all tested frequencies, significant increase in ATP production of NP cells was only seen at 1 Hz dynamic frequency. This observation is consistent with a previous study conducted by

Maclean et al. where in vivo dynamic compression of discs showed that AF cellular response was primarily dependent on magnitude than frequency, and NP cells were sensitive to both loading amplitude and frequency [58]. The differential response between cell types can be attributed to their intrinsic differences which are adaptations to their unique environment and functionality. Furthermore, this data presents an interaction between loading frequency and magnitude. Similar interaction was reported by Maclean et al. for AF cells [58]. However, in that study, dynamic compression stimulated a catabolic response in AF cells at their tested conditions. Wang et al. subjected rabbit IVD explants to dynamic loading at two strain levels [88]. In that study both cell types showed an anabolic response to dynamic loading with possible interactions due to loading parameters. Another study conducted by Kasra et al examined the effects of dynamic hydrostatic pressure on rabbit IVD cells (AF cells - monolayer culturing; NP cells seeded in alginate constructs) [45]. Here collagen and protein metabolism was evaluated at a wide frequency range, 1 – 20 Hz at different magnitudes. They reported that at high amplitude and high frequency, collagen synthesis was promoted in AF cells but had no effect on proteases responsible for AF ECM breakdown; in NP cells however, in addition to increased biosynthesis, down regulation of degradation enzyme activity was also detected. Additionally neither cell type was stimulated at low amplitude and frequencies. It is apparent that direct comparisons between various studies are difficult due to significant amount of variables associated with each protocol. However, overall, it can be said that cellular biosynthesis is regulated by mechanical loading and the net effect is highly dependent on loading parameters. Our study illustrates that mechanical loading affects ATP production of IVD cells. Thus the

change in ATP production might be a governing factor for altered cellular biosynthesis under mechanical loading.

5.2.3: ATP release due to mechanical loading

In this study, higher dynamic loading frequencies (1, 2 Hz) exhibited a significant increase in ATP release from both AF and NP cells. However, only NP cells exhibited frequency dependence in this response. Additionally, NP cells under 30% static compression stimulated an increase in ATP release. ATP released from AF cells was not responsive to static compression at either of the strain levels. This data indicates that ATP release is up-regulated by higher dynamic compression frequencies and higher static strain magnitudes.

ATP release due to mechanical stimulation has been observed in various cell types [27,50]. A study conducted by Graff et al showed that chondron pellets significantly up-regulated ATP release under mechanical stimulation but cells exhibited desensitization to continuous loading [19]. Another study conducted on AF cells showed maximum ATP release after 10 min and 30 min of continued vibratory loading for human and rat cells respectively [90]. Similarly to Graff et al, Yamazaki et al study found that continued mechanical stimulation results in below control ATP levels. However, it is important to note that the above mentioned studies were conducted at different culture conditions (pellet culture, monolayer culture respectively) which may contribute to the final response. Additionally, these studies allowed longer culture periods to promote extracellular matrix build up.

The physiological role of ATP release due to mechanical stimulation was not evaluated in this study. However, studies have shown that extracellular ATP and its metabolites are able to regulate cellular biosynthesis [13,16,19,64]. Additionally, studies have shown that inorganic pyrophosphate (PPi), an ATP metabolite is able to induce cartilage calcification [31,43,78]. Though may not be its primary function, ATP release in response to various mechanical stimulations of the spine, may inadvertently promote calcification of the cartilaginous end plate over time. As such, this may be a primary pathway for age dependent CEP calcification and subsequent disc degeneration due to resulting decreased nutrient supply.

ATP at increased extracellular concentrations have also been implicated in activating nociceptive nerves [14,15]. Although avascular and aneural in healthy adult disc, nerve in-growth and vasculature occurs with degeneration [18]. While a high extracellular ATP concentration is required for this stimulation, this threshold can be decreased if the microenvironment acidifies [53]. Accumulation of lactic acid could occur in degenerated discs due to decreased tissue diffusivity providing the necessary conditions to stimulate pain nerves within the degenerated discs. As such, this may provide a link between sensation of low back pain and disc degeneration. Additionally, intracellular ATP concentration is approximately 1000-fold higher compared to extracellular ATP [17]. Cell death which may occur due to high impact loading and during disc degeneration will result in significant increase in extracellular ATP and further contribute to activation of pain receptors.

5.2.3: NO production due to mechanical loading

Static and dynamic loading of NP cells significantly up regulated NO production. NO production of AF cells was increased by higher dynamic frequencies (1 Hz and 2 Hz) but not by static compression or 0.1 Hz dynamic frequency. These data clearly demonstrate that mechanical stimulation affects NO production in IVD cells and further that these cells are affected differently.

Contrary to the down regulation of NO production observed in dynamic compression of bovine chondrocytes conducted by Lee et al. [51], in our study, NO production was either up regulated or unaffected by mechanical loading. This variation in response can be attributed to intrinsic differences between chondrocytes, AF and NP cell types. Significant difference in the experiment duration, 4 h vs. 48 h, might also have an effect on the final concentrations and as such conclusions. Furthermore, mechanically stimulated NO production of chondrocytes is considered to be regulated by a purinergic pathway [13]. Though not conclusive due to lack of inhibition testing, our data display a significant correlation between NO production and ATP release due to mechanical stimulation. Thus further investigations must be conducted to identify the physiological significance of this observation.

Tomita et al. evaluated the effects of NO on energy metabolism on articular chondrocytes at oxygen tensions 5% and 20% [83]. They concluded that respiration and ATP synthesis was inhibited by NO and increase in extracellular NO concentration enhanced glucose consumption and lactate production. Although our data are explained with the hypothesis that under tested conditions, NP cells primarily utilize mitochondrial

respiration for ATP production, further experiments with complete inhibition of mitochondrial respiration are required to prove this hypothesis.

5.2.3: Differential response of AF and NP cells under mechanical loading

At control and all tested conditions glucose consumption and lactate production of NP cells were significantly lower to that to AF cells. However, total ATP cell content remained significantly higher in NP cells for control and all experiment groups. Collectively this finding suggests that at performed culture conditions (25mM glucose DMEM; 20% O_2), NP cell ATP synthesis was dominated by mitochondrial respiration. A study conducted by Huang et al demonstrated that oxygen consumption of NP cells was significantly higher to that of AF cells [35]. A similar observation was made by Ishihara et al, in which increased oxygen tension decreased lactate production of IVD discs [38]. In the current study, although significantly lower, NP cells exhibited lactate production in the range of 41% - 69% relative to AF cells. This indicates that ATP production of NP cells in not exclusive to aerobic respiration. Relatively lower NO production in NP cells observed throughout all experiment groups could possibly be due to tight regulation of NO production in NP cells to retain aerobic respiration. Additionally it should be noted, that the immature NP cells used in our experiment is more similar to notochordal cells. Thus, mature NP cells might respond differently to these mechanical stimulations. Furthermore, higher NO production observed in AF cells might limit (or prevent) ATP synthesis via mitochondrial respiration which could explain relatively lower ATP synthesis in AF cells.

There were no significant differences in ATP release between AF and NP cells at control and 1 Hz culture conditions. NP cell ATP release was significantly higher to those of AF cells under static compression (15% and 30%) and 2 Hz dynamic loading. 0.1 Hz dynamic compression however exhibited a reversed response in which AF cells released more ATP relative to NP cells. Overall, this finding suggests with the exception of low dynamic loading frequency, NP cells have a significantly higher contribution to extracellular ATP concentrations than AF cells. The physiological significance of this effect remains to be investigated. However, as mentioned previously, chondrocytes studies have illustrated the effects of extracellular ATP on cartilage calcification. As such, the permeable region of CEP which calcifies with aging maybe initiated by ATP released from IVD cells. Furthermore, these observations collectively highlight the intrinsic differences in AF and NP cells and their differential cellular responses based on applied stimulation.

5.3 Experiment limitations

The present study was conducted to evaluate the effects of various mechanical loading parameters on energy metabolism of IVD cells. It is apparent based on numerous studies cited here, that cellular response is affected by mechanical stimulation, yet the exact reaction is significantly affected by the loading regimen. Therefore direct comparison among various studies is difficult due to different loading parameters (strain level, loading type and duration) and experimental protocols (tissue, explants and cells) which in combination will produce differential responses.

A recent study demonstrated that osmolarity of tissue/culture system has a significant impact on cellular response to mechanical stimulation [86]. Additionally, a study conducted on effects of oxygen tension on NO production showed that biological effects of NO was more pronounced at, low or in vivo oxygen tensions. Our study was conducted at iso-osmolar conditions at 21% oxygen tension in 25 mM glucose concentrations. Further investigations simulating in vivo osmolarity, glucose and oxygen tensions will provide us data that is more comparable to in vivo cellular responses.

Chapter 6: CONCLUSION AND FUTURE WORK

Previous studies have investigated the effects of mechanical loading on IVD biosynthesis. This is the first study to evaluate the effects of static compressive mechanical loading and multiple compressive dynamic loading frequencies on energy metabolism of IVD cells. Here we report that IVD cell energy metabolism is altered by mechanical loading. ATP production of AF Cells was promoted at all tested compressions (dynamic and static). However, increased ATP production of NP cells was only detected at 1 Hz. Furthermore, the data indicates that IVD cells respond differently to the same mechanical stimulation highlighting its intrinsic differences. Additionally, comparison between AF and NP cells strongly suggests that NP cells utilize aerobic respiration as a major part of its energy production pathway.

In future studies, protein synthesis must also be evaluated under mechanical loading to confirm that increased energy production is utilized for cellular biosynthesis activities. Given this study was conducted at 21% O_2 in 25 mM glucose, in vivo cellular response may differ from the observations in this study. Thus future studies must evaluate the effects of mechanical loading in culture condition parameters that mimic in vivo conditions. Additionally, NP cells used in this study are notochordal (immature) cells. Therefore, future studies must evaluate the effects of mechanical loading on mature NP cells, which is likely to respond differently.

Significant increase in ATP release due to mechanical loading was observed in this study. Previous studies on chondrocytes have reported that extracellular ATP affects extracellular matrix synthesis and cartilage calcification. Therefore, future studies will be conducted to evaluate if extracellular ATP has a similar effects on IVD tissue.

REFERENCES

[1] American Academy of orthopedics surgeons. The burden of musculoskeletal diseases in the united states. The Bone and Joint Decade 2008; 21-53

[2] Apodaca G. Modulation of membrane traffic by mechanical stimuli. Am J Physiol Renal Physiol 2002; 282 F179-F190

[3] Battie MC, Videman T, Gibbons LE, et al. 1995 Volvo Award in clinical sciences. Determinants of lumbar disc degeneration. A study relating lifetime exposures and magnetic resonance imaging findings in identical twins. Spine (Phila Pa 1976) 1995; 20 2601-12

[4] Bibby SR, Fairbank JC, Urban MR, Urban JP. Cell viability in scoliotic discs in relation to disc deformity and nutrient levels. Spine (Phila Pa 1976) 2002; 27 2220-8

[5] Bibby SR, Jones DA, Ripley RM, Urban JP. Metabolism of the intervertebral disc: effects of low levels of oxygen, glucose, and pH on rates of energy metabolism of bovine nucleus pulposus cells. Spine (Phila Pa 1976) 2005; 30 487-96

[6] Bibby SR, Urban JP. Effect of nutrient deprivation on the viability of intervertebral disc cells. Eur Spine J 2004; 13 695-701

[7] Blanco FJ, Lotz M. IL-1-induced nitric oxide inhibits chondrocyte proliferation via PGE2. Exp Cell Res 1995; 218 319-25

[8] Brookes PS, Bolanos JP, Heales SJ. The assumption that nitric oxide inhibits mitochondrial ATP synthesis is correct. FEBS Lett 1999; 446 261-3

[9] Brown GC. Nitric oxide regulates mitochondrial respiration and cell functions by inhibiting cytochrome oxidase. FEBS Lett 1995; 369 136-9

[10] Buckwalter JA. Aging and degeneration of the human intervertebral disc. Spine (Phila Pa 1976) 1995; 20 1307-14

[11] Chou AI, Bansal A, Miller GJ, Nicoll SB. The effect of serial monolayer passaging on the collagen expression profile of outer and inner anulus fibrosus cells. Spine (Phila Pa 1976) 2006; 31 1875-81

[12] Chou AIB, Bansal AB, Miller GJB, Nicoll SB. The Effect of Serial Monolayer Passaging on the Collagen Expression Profile of Outer and Inner Anulus Fibrosus Cells. Spine 2006; 31 1875-81

[13] Chowdhury TT, Knight MM. Purinergic pathway suppresses the release of .NO and stimulates proteoglycan synthesis in chondrocyte/agarose constructs subjected to dynamic compression. J Cell Physiol 2006; 209 845-53

[14] Dowd E, McQueen DS, Chessell IP, Humphrey PP. P2X receptor-mediated excitation of nociceptive afferents in the normal and arthritic rat knee joint. Br J Pharmacol 1998; 125 341-6

[15] Dowd E, McQueen DS, Chessell IP, Humphrey PP. Adenosine A1 receptor-mediated excitation of nociceptive afferents innervating the normal and arthritic rat knee joint. Br J Pharmacol 1998; 125 1267-71

[16] Elfervig MK, Graff RD, Lee GM, et al. ATP induces Ca(2+) signaling in human chondrons cultured in three-dimensional agarose films. Osteoarthritis Cartilage 2001; 9 518-26

[17] Fitz JG. Regulation of cellular ATP release. Trans Am Clin Climatol Assoc 2007; 118 199-208

[18] Freemont AJ. The cellular pathobiology of the degenerate intervertebral disc and discogenic back pain. Rheumatology (Oxford) 2009; 48 5-10

[19] Graff RD, Lazarowski ER, Banes AJ, Lee GM. ATP release by mechanically loaded porcine chondrons in pellet culture. Arthritis Rheum 2000; 43 1571-9

[20] Granger DL, Anstey NM, Miller WC, Weinberg JB. Measuring nitric oxide production in human clinical studies. Methods Enzymol 1999; 301 49-61

[21] Gruber HE, Fisher EC, Jr., Desai B, et al. Human intervertebral disc cells from the annulus: three-dimensional culture in agarose or alginate and responsiveness to TGF-beta1. Exp Cell Res 1997; 235 13-21

[22] Gruber HE, Leslie K, Ingram J, et al. Colony formation and matrix production by human anulus cells: modulation in three-dimensional culture. Spine (Phila Pa 1976) 2004; 29 E267-E274

[23] Gu WY, Yao H, Huang CY, Cheung HS. New insight into deformation-dependent hydraulic permeability of gels and cartilage, and dynamic behavior of agarose gels in confined compression. J Biomech 2003; 36 593-8

[24] Gu WY, Yao H, Vega AL, Flagler D. Diffusivity of ions in agarose gels and intervertebral disc: effect of porosity. Ann Biomed Eng 2004; 32 1710-7

[25] Guehring T, Wilde G, Sumner M, et al. Notochordal intervertebral disc cells: sensitivity to nutrient deprivation. Arthritis Rheum 2009; 60 1026-34

[26] Handa T, Ishihara H, Ohshima H, et al. Effects of hydrostatic pressure on matrix synthesis and matrix metalloproteinase production in the human lumbar intervertebral disc. Spine (Phila Pa 1976) 1997; 22 1085-91

[27] Harden TK, Lazarowski ER, Boucher RC. Release, metabolism and interconversion of adenine and uridine nucleotides: implications for G protein-coupled P2 receptor agonist selectivity. Trends Pharmacol Sci 1997; 18 43-6

[28] Hill TE, Desmoulin GT, Hunter CJ. Is vibration truly an injurious stimulus in the human spine? J Biomech 2009; 42 2631-5

[29] Hishikawa K, Luscher TF. Pulsatile stretch stimulates superoxide production in human aortic endothelial cells. Circulation 1997; 96 3610-6

[30] Horner HA, Roberts S, Bielby RC, et al. Cells from different regions of the intervertebral disc: effect of culture system on matrix expression and cell phenotype. Spine (Phila Pa 1976) 2002; 27 1018-28

[31] Hsu HH, Anderson HC. Calcification of isolated matrix vesicles and reconstituted vesicles from fetal bovine cartilage. Proc Natl Acad Sci U S A 1978; 75 3805-8

[32] Huang CY, Gu WY. Effects of mechanical compression on metabolism and distribution of oxygen and lactate in intervertebral disc. J Biomech 2008; 41 1184-96

[33] Huang CY, Hagar KL, Frost LE, et al. Effects of cyclic compressive loading on chondrogenesis of rabbit bone-marrow derived mesenchymal stem cells. Stem Cells 2004; 22 313-23

[34] Huang CY, Reuben PM, Cheung HS. Temporal expression patterns and corresponding protein inductions of early responsive genes in rabbit bone marrow-derived mesenchymal stem cells under cyclic compressive loading. Stem Cells 2005; 23 1113-21

[35] Huang CY, Yuan TY, Jackson AR, et al. Effects of low glucose concentrations on oxygen consumption rates of intervertebral disc cells. Spine (Phila Pa 1976) 2007; 32 2063-9

[36] Hutton WC, Elmer WA, Boden SD, et al. The effect of hydrostatic pressure on intervertebral disc metabolism. Spine (Phila Pa 1976) 1999; 24 1507-15

[37] Ishihara H, McNally DS, Urban JP, Hall AC. Effects of hydrostatic pressure on matrix synthesis in different regions of the intervertebral disk. J Appl Physiol 1996; 80 839-46

[38] Ishihara H, Urban JP. Effects of low oxygen concentrations and metabolic inhibitors on proteoglycan and protein synthesis rates in the intervertebral disc. J Orthop Res 1999; 17 829-35

[39] Jackson AR, Yuan TY, Huang CY, et al. Effect of compression and anisotropy on the diffusion of glucose in annulus fibrosus. Spine (Phila Pa 1976) 2008; 33 1-7

[40] Javedan SP, Dickman CA. Cause of adjacent-segment disease after spinal fusion. Lancet 1999; 354 530-1

[41] Johnson DL, McAllister TN, Frangos JA. Fluid flow stimulates rapid and continuous release of nitric oxide in osteoblasts. Am J Physiol 1996; 271 E205-E208

[42] Johnson K, Svensson CI, Etten DV, et al. Mediation of spontaneous knee osteoarthritis by progressive chondrocyte ATP depletion in Hartley guinea pigs. Arthritis Rheum 2004; 50 1216-25

[43] Johnson K, Terkeltaub R. Inorganic pyrophosphate (PPI) in pathologic calcification of articular cartilage. Front Biosci 2005; 10 988-97

[44] Johnson WE, Caterson B, Eisenstein SM, et al. Human intervertebral disc aggrecan inhibits nerve growth in vitro. Arthritis Rheum 2002; 46 2658-64

[45] Kasra M, Goel V, Martin J, et al. Effect of dynamic hydrostatic pressure on rabbit intervertebral disc cells. J Orthop Res 2003; 21 597-603

[46] Kauppila LI. Prevalence of stenotic changes in arteries supplying the lumbar spine. A postmortem angiographic study on 140 subjects. Ann Rheum Dis 1997; 56 591-5

[47] Kauppila LI, McAlindon T, Evans S, et al. Disc degeneration/back pain and calcification of the abdominal aorta. A 25-year follow-up study in Framingham. Spine (Phila Pa 1976) 1997; 22 1642-7

[48] Kim PK, Branch CL, Jr. The lumbar degenerative disc: confusion, mechanics, management. Clin Neurosurg 2006; 53 18-25

[49] Kumar A, Varghese M, Mohan D, et al. Effect of whole-body vibration on the low back. A study of tractor-driving farmers in north India. Spine (Phila Pa 1976) 1999; 24 2506-15

[50] Lazarowski ER, Homolya L, Boucher RC, Harden TK. Direct demonstration of mechanically induced release of cellular UTP and its implication for uridine nucleotide receptor activation. J Biol Chem 1997; 272 24348-54

[51] Lee DA, Frean SP, Lees P, Bader DL. Dynamic mechanical compression influences nitric oxide production by articular chondrocytes seeded in agarose. Biochem Biophys Res Commun 1998; 251 580-5

[52] Lee RB, Wilkins RJ, Razaq S, Urban JP. The effect of mechanical stress on cartilage energy metabolism. Biorheology 2002; 39 133-43

[53] Li C, Peoples RW, Weight FF. Proton potentiation of ATP-gated ion channel responses to ATP and Zn2+ in rat nodose ganglion neurons. J Neurophysiol 1996; 76 3048-58

[54] Lipson SJ, Muir H. Experimental intervertebral disc degeneration: morphologic and proteoglycan changes over time. Arthritis Rheum 1981; 24 12-21

[55] Livak KJ, Schmittgen TD. Analysis of relative gene expression data using real-time quantitative PCR and the 2(-Delta Delta C(T)) Method. Methods 2001; 25 402-8

[56] Lotz JC, Colliou OK, Chin JR, et al. Compression-induced degeneration of the intervertebral disc: an in vivo mouse model and finite-element study. Spine (Phila Pa 1976) 1998; 23 2493-506

[57] MacLean JJ, Lee CR, Alini M, Iatridis JC. The effects of short-term load duration on anabolic and catabolic gene expression in the rat tail intervertebral disc. J Orthop Res 2005; 23 1120-7

[58] MacLean JJ, Lee CR, Alini M, Iatridis JC. Anabolic and catabolic mRNA levels of the intervertebral disc vary with the magnitude and frequency of in vivo dynamic compression. J Orthop Res 2004; 22 1193-200

[59] Maldonado BA, Oegema TR, Jr. Initial characterization of the metabolism of intervertebral disc cells encapsulated in microspheres. J Orthop Res 1992; 10 677-90

[60] Marchand F, Ahmed AM. Investigation of the laminate structure of lumbar disc anulus fibrosus. Spine (Phila Pa 1976) 1990; 15 402-10

[61] Maroudas A. Biophysical chemistry of cartilaginous tissues with special reference to solute and fluid transport. Biorheology 1975; 12 233-48

[62] Maroudas A, Stockwell RA, Nachemson A, Urban J. Factors involved in the nutrition of the human lumbar intervertebral disc: cellularity and diffusion of glucose in vitro. J Anat 1975; 120 113-30

[63] Mauck RL, Byers BA, Yuan X, Tuan RS. Regulation of cartilaginous ECM gene transcription by chondrocytes and MSCs in 3D culture in response to dynamic loading. Biomech Model Mechanobiol 2007; 6 113-25

[64] Millward-Sadler SJ, Wright MO, Flatman PW, Salter DM. ATP in the mechanotransduction pathway of normal human chondrocytes. Biorheology 2004; 41 567-75

[65] Mwale F, Roughley P, Antoniou J. Distinction between the extracellular matrix of the nucleus pulposus and hyaline cartilage: a requisite for tissue engineering of intervertebral disc. Eur Cell Mater 2004; 8 58-63

[66] Noris M, Morigi M, Donadelli R, et al. Nitric oxide synthesis by cultured endothelial cells is modulated by flow conditions. Circ Res 1995; 76 536-43

[67] Oegema TR, Jr. Biochemistry of the intervertebral disc. Clin Sports Med 1993; 12 419-39

[68] Oegema TR, Jr., Johnson SL, Aguiar DJ, Ogilvie JW. Fibronectin and its fragments increase with degeneration in the human intervertebral disc. Spine (Phila Pa 1976) 2000; 25 2742-7

[69] Ohshima H, Urban JP, Bergel DH. Effect of static load on matrix synthesis rates in the intervertebral disc measured in vitro by a new perfusion technique. J Orthop Res 1995; 13 22-9

[70] Osti OL, Vernon-Roberts B, Fraser RD. 1990 Volvo Award in experimental studies. Anulus tears and intervertebral disc degeneration. An experimental study using an animal model. Spine (Phila Pa 1976) 1990; 15 762-7

[71] Peng BG, Wu WW, Hou SX, et al. [The pathogenesis of discogenic low back pain]. Zhonghua Wai Ke Za Zhi 2004; 42 720-4

[72] Pitsillides AA, Rawlinson SC, Suswillo RF, et al. Mechanical strain-induced NO production by bone cells: a possible role in adaptive bone (re)modeling? FASEB J 1995; 9 1614-22

[73] Putzier M, Schneider SV, Funk JF, et al. The surgical treatment of the lumbar disc prolapse: nucleotomy with additional transpedicular dynamic stabilization versus nucleotomy alone. Spine (Phila Pa 1976) 2005; 30 E109-E114

[74] Quinn TM, Kocian P, Meister JJ. Static compression is associated with decreased diffusivity of dextrans in cartilage explants. Arch Biochem Biophys 2000; 384 327-34

[75] Raj PP. Intervertebral disc: anatomy-physiology-pathophysiology-treatment. Pain Pract 2008; 8 18-44

[76] Ranu HS. Measurement of pressures in the nucleus and within the annulus of the human spinal disc: due to extreme loading. Proc Inst Mech Eng H 1990; 204 141-6

[77] Roberts S, Eisenstein SM, Menage J, et al. Mechanoreceptors in intervertebral discs. Morphology, distribution, and neuropeptides. Spine (Phila Pa 1976) 1995; 20 2645-51

[78] Ryan LM, Kurup IV, Derfus BA, Kushnaryov VM. ATP-induced chondrocalcinosis. Arthritis Rheum 1992; 35 1520-5

[79] Sambrook PN, MacGregor AJ, Spector TD. Genetic influences on cervical and lumbar disc degeneration: a magnetic resonance imaging study in twins. Arthritis Rheum 1999; 42 366-72

[80] Setton LA, Chen J. Cell mechanics and mechanobiology in the intervertebral disc. Spine (Phila Pa 1976) 2004; 29 2710-23

[81] Setton LA, Chen J. Mechanobiology of the intervertebral disc and relevance to disc degeneration. J Bone Joint Surg Am 2006; 88 Suppl 2 52-7

[82] Taskiran D, Stefanovic-Racic M, Georgescu H, Evans C. Nitric oxide mediates suppression of cartilage proteoglycan synthesis by interleukin-1. Biochem Biophys Res Commun 1994; 200 142-8

[83] Tomita M, Sato EF, Nishikawa M, et al. Nitric oxide regulates mitochondrial respiration and functions of articular chondrocytes. Arthritis Rheum 2001; 44 96-104

[84] Trout JJ, Buckwalter JA, Moore KC. Ultrastructure of the human intervertebral disc: II. Cells of the nucleus pulposus. Anat Rec 1982; 204 307-14

[85] Trout JJ, Buckwalter JA, Moore KC, Landas SK. Ultrastructure of the human intervertebral disc. I. Changes in notochordal cells with age. Tissue Cell 1982; 14 359-69

[86] Urban JP. The role of the physicochemical environment in determining disc cell behaviour. Biochem Soc Trans 2002; 30 858-64

[87] Urban JP, Smith S, Fairbank JC. Nutrition of the intervertebral disc. Spine (Phila Pa 1976) 2004; 29 2700-9

[88] Wang DL, Jiang SD, Dai LY. Biologic response of the intervertebral disc to static and dynamic compression in vitro. Spine (Phila Pa 1976) 2007; 32 2521-8

[89] Yamazaki S, Banes AJ, Weinhold PS, et al. Vibratory loading decreases extracellular matrix and matrix metalloproteinase gene expression in rabbit annulus cells. Spine J 2002; 2 415-20

[90] Yamazaki S, Weinhold PS, Graff RD, et al. Annulus cells release ATP in response to vibratory loading in vitro. J Cell Biochem 2003; 90 812-8

[91] Yuan TY, Jackson AR, Huang CY, Gu WY. Strain-dependent oxygen diffusivity in bovine annulus fibrosus. J Biomech Eng 2009; 131 074503